

UCSF

UC San Francisco Electronic Theses and Dissertations

Title

The role of visual area MT in oculomotor behavior

Permalink

<https://escholarship.org/uc/item/5r74s4gm>

Author

Hohl, Sonja Seraina

Publication Date

2011

Peer reviewed|Thesis/dissertation

The role of visual area MT in oculomotor behavior

by

Sonja Seraina Hohl

DISSERTATION

Submitted in partial satisfaction of the requirements for the degree of

DOCTOR OF PHILOSOPHY

in

Neuroscience

in the

GRADUATE DIVISION

Copyright 2011

by

Sonja Seraina Hohl Mante

Dedication

I would like to dedicate this thesis to two people who were very dear to me and passed away during my graduate career.

To my father, Peter Edward Hohl. From you I inherited my love of nature. I think of you every time I see beautiful birds perched on the branches outside our windows. We shared a common sense of humor and often laughed tears together. You gave me strength by believing in me. I will always miss you.

To my grandmother Emma Mueller. Your support throughout my undergraduate studies meant so much to me. We both loved art and often went to the movies together. You wanted to see my newest paintings and projects I was working on. Last but not least you understood my academic curiosity. Although you were over 90 years old, you made me explain my research to you over and over again. A few weeks before your death you told me you'd like to read my thesis. I'm sorry I wasn't able to finish fast enough.

Acknowledgments

First and foremost I would like to thank Steve Lisberger for having me in his lab. I have always wanted to understand everything down to the smallest detail and surely my training as a physicist has reinforced this trait. In life sciences, however, problems are too complex to solve in such detail. Steve has endlessly tried to redirect my approach of solving problems to seeing ‘the forest’ instead of ‘the trees’. I hope some of your efforts have rubbed off on me. Steve is an exceptional role model in so many ways, scientific and personal. His influence will surely provide constant guidance throughout my career, wherever it may lead.

I wish to thank my lab mates, my office mates, the Keck Center, and my thesis committee members for providing a stimulating intellectual environment. I will thoroughly miss the exchange of ideas and discussions that have shaped this work. This community has expanded my way of thinking from that of a physicist to that of a neuroscientist.

Without the technical support of Stefanie Tokiyama, Liz Montgomery, Karen Macleod, Ned Molyneaux, Scott Ruffner, Dirk Kleinhesselink, David Wolfgang-Kimball, Laszlo Bocscai, Daryll Floyd, and Ken McGary, none of this work would have been possible.

Many friends have provided incredible and much needed support throughout graduate school. I couldn’t have done this without you. In particular, there is no way to

express my gratitude towards Archana Shenoy, Anna Ma-Wyatt, and Hilary Heuer for encouraging me and always being there for me.

I am extremely grateful to my siblings Tobias, Corinne, and Annik, my parents Peter and Annemarie, and grandmothers Emma and Joan who have made me the person who I am and enriched my life in every aspect. You have supported me so patiently throughout graduate school. I look forward to many more rounds of Settlers and Jass once this thesis is handed in!

Last, but not least, my husband Valerio Mante is the best partner I could wish for. Thank you for everything. Our bundle of joy, Janine, has provided wonderful distraction from the stress of writing this thesis. I look forward to many adventures with our little family.

Abstract

For many behaviors we rely on our senses, which inform the brain about the world around us, such as the spatial location of an object we would like to grasp or the motion of a target that we intend to follow with our eyes. In order to execute an appropriate movement, neural responses in sensory areas must be read out and transformed into signals meaningful to premotor and motor areas so an accurate motor command can evolve. I used smooth pursuit eye movements to study the sensory-motor transformation of visual signals about object motion into an appropriate motor command for accelerating the eyes. I found that fluctuations in single neuron responses in visual area MT are predictive of deviations in eye speed during pursuit initiation, which suggests that responses in MT contribute to noise in the motor output. Further, the relationship between the sensory and motor variability revealed constraints about the neural mechanisms underlying the transformation of MT signals into a command for eye speed: if downstream noise is low, a modified vector averaging computation involving opponent signals between oppositely tuned neurons could explain the relationship between responses of single neurons in area MT and eye speed at the initiation of pursuit.

In addition to smooth pursuit eye movements, we studied MT responses during drifts in eye movements of fixation. I found that deviations in sensory responses not only predict variation in pursuit initiation, but that deviations in eye velocity during fixation also modulate the neural responses in MT. I showed that firing rates in MT are modulated because tiny changes in eye velocity generate image motion on the retina. These results

demonstrate that image motion due to miniature eye movements is large enough to affect the responses of visual neurons beyond the retina or early cortical visual areas.

This thesis has underscored how tightly sensory and motor systems are interwoven; visual area MT, in particular, forms an important link between the processing of visual signals and the generation of motor commands for smooth pursuit eye movements.

Table of contents

Dedication	iii
Acknowledgments	iv
Abstract	vi
Table of contents	viii
List of figures	x
Chapter 1: General Introduction.....	1
References.....	6
Chapter 2: Responses to perceptually invisible image motion in extrastriate visual area MT in macaque monkeys.....	8
Abstract.....	9
Introduction.....	10
Materials and Methods	14
Results.....	20
Discussion	39
References.....	44
Chapter 3: Noise correlations between responses of MT neurons and initiation of smooth pursuit eye movements	52
Abstract.....	53
Introduction.....	54
Materials and Methods	58
Results.....	69
Discussion.....	91

References.....	97
Chapter 4: Appendix.....	104
Linear predictions of pursuit eye velocity	105
References.....	114
Chapter 5: Conclusions and Future Directions	115
References.....	120

List of figures

Chapter 2: Responses to perceptually invisible image motion in extrastriate visual area

MT in macaque monkeys

Figure 2.1	20
Figure 2.2	22
Figure 2.3	24
Figure 2.4	26
Figure 2.5	27
Figure 2.6	29
Figure 2.7	31
Figure 2.8	33
Figure 2.9	35
Figure 2.10	37

Chapter 3: Noise correlations between responses of MT neurons and initiation of smooth

pursuit eye movements

Figure 3.1	70
Figure 3.2	71
Figure 3.3	73
Figure 3.4	75

Figure 3.5.....	79
Figure 3.6.....	83
Figure 3.7.....	86
Figure 3.8.....	88

Chapter 4: Appendix

Figure 4.1.....	106
Figure 4.2.....	108
Figure 4.3.....	111

Chapter 1: General Introduction

Vision is an active process by which we take up information about our environment. We see because light enters the eyes through the pupils and reaches the retina. On the retina cells that are photosensitive convert light into electrical signals that inform the brain about our visual environment. These signals are processed by various sub-cortical and cortical structures to provide the basis for visual perception. The physical properties of our eyes such as the diameter of the pupil limit the visual field, which is the extent of the environment from which we can absorb photons and therefore see. While the visual field is quite wide, humans and primates have highly accurate vision only in a small region at the center of the visual field called the fovea. As a consequence, humans and primates actively use a combination of head and eye movements to direct their foveae to objects of interest. Eye movements not only increase our visual range, they are also implicated in various other important functions enhancing our visual abilities.

Eye movements affect vision by shifting the image that falls onto the retina and vision in turn guides eye movements by providing information about the visual environment. This complex interaction between the visual and oculomotor system is essential for guiding active vision, yet the neural mechanisms underlying this interaction remain poorly understood. In this thesis, in an effort to explore the integration of the visual and oculomotor systems, I first investigated how small eye movements during fixation affect sensory processing of visual inputs in chapter 2. In chapter 3 I investigated how sensory signals constrain motor performance during smooth pursuit eye movements.

The oculomotor system provided an excellent model system to investigate complex interactions between sensory signals and motor behavior. Eye movements are a

simple motor behavior as the eyes are each controlled by only 6 muscles. The pathways controlling eye movements and those, for example, controlling reaching have common properties and therefore our knowledge of the oculomotor system might lead to a deeper understanding of more complex behaviors such as reaching arm movements (Lisberger, 2010). In addition to serving as a model system, eye movements themselves are highly relevant because both humans and primates rely heavily on vision to interact with the environment.

Eye movements of fixation are small involuntary movements that play an important functional role in maintaining vision (Martinez-Conde, Macknik, & Hubel, 2004). They occur during instances when we hold our gaze still and we are completely unaware of them. Drifts, in particular, are the slow, low frequency eye movements occurring during fixation (Adler & Fliegelman, 1934; Ratliff & Riggs, 1950; Skavenski, Robinson, Steinman, & Timberlake, 1975). Visual neurons decrease their responses when the visual input is constant over a period of time. This adaptation of neural responses leads to perceptual fading when a visual image lies still on the retina (Ditchburn & Ginsborg, 1952). Eye movements during fixation prevent adaptation of visual neurons and therefore fading by jittering a stationary image on the retina.

Although the eye movements of fixation are important for enabling normal vision, they generate image motion on the retina, which the brain must convert into a stationary perception of the world. It is unclear how the brain compensates for these visual motion signals and at what level of visual processing this compensation occurs. An important step towards understanding the neural mechanisms underlying perceptual stabilization is

to learn how neurons in different visual areas respond during eye movements of fixation and how these signals could be used to eliminate global motion of the visual world.

Neurons in extrastriate area MT are sensitive to motion in a visual stimulus and I therefore investigated whether these neurons are modulated specifically by the small image motions generated by drifts. MT neurons signal the direction and speed of visual motion (Albright, 1984; Maunsell & Van Essen, 1983) and their responses have been shown to influence the perception of motion (Britten, Newsome, Shadlen, Celebrini, & Movshon, 1996; Salzman, Britten, & Newsome, 1990; Zohary, Shadlen, & Newsome, 1994). Although this visual area had been studied extensively in the past, it had almost exclusively been investigated using motion stimuli much faster than the image motion generated by drifts. In my recordings, I found that MT neurons clearly respond during drifts in a direction-specific way. These neural signals in MT could potentially play an important role in the compensation for retinal motion generated by eye movements during fixation. My results demonstrate that motion signals during fixation are not eliminated in early visual areas as had been suggested in previous studies. These findings are an important step in establishing the contribution of early visual areas and MT in discounting motion induced by drifts. They must be taken into account in future models explaining perceptual stabilization of image motion generated by fixational eye movements.

Chapter 3 investigated the role of visual signals in generating smooth pursuit eye movements. Smooth pursuit eye movements are the voluntary movements that allow us to keep the image of a moving target centered on our foveae. The smooth pursuit system relies on the visual motion input provided by area MT to estimate the speed and direction

of a moving target. It then transforms these motion signals into an appropriate motor command for the eye muscles so the speed and direction of the eyes match the target motion.

Measuring correlations between fluctuations in neural and behavioral responses revealed a close link between sensory area MT and pursuit behavior. Our results suggest that fluctuations in visual motion signals provided by MT affect the eye speed of pursuit and thereby contribute to noise in the motor output. Further, the correlations we measured provide a significant and novel insight into possible mechanisms by which sensory signals from MT are transformed to yield an accurate motor command for pursuit.

We have demonstrated that miniature eye movements modulate sensory responses and that these, in turn, predict variability in motor behavior on a trial-by-trial basis. These findings show how intricately sensory and motor systems are linked in the neural processing of visual signals and the production of oculomotor behavior. Our recordings of single neural responses suggest that visual area MT might play a central role in the neural mechanisms underpinning active vision.

References

- Adler, F. A., & Fliegelman, M. (1934). Influence of fixation on the visual acuity. *Arch Ophthalmol*, 12, 475-483.
- Albright, T. D. (1984). Direction and orientation selectivity of neurons in visual area MT of the macaque. *J Neurophysiol*, 52(6), 1106-1130.
- Britten, K. H., Newsome, W. T., Shadlen, M. N., Celebrini, S., & Movshon, J. A. (1996). A relationship between behavioral choice and the visual responses of neurons in macaque MT. *Vis Neurosci*, 13(1), 87-100.
- Ditchburn, R. W., & Ginsborg, B. L. (1952). Vision with a stabilized retinal image. *Nature*, 170(4314), 36-37.
- Lisberger, S. G. (2010). Visual guidance of smooth-pursuit eye movements: sensation, action, and what happens in between. *Neuron*, 66(4), 477-491.
- Martinez-Conde, S., Macknik, S. L., & Hubel, D. H. (2004). The role of fixational eye movements in visual perception. *Nat Rev Neurosci*, 5(3), 229-240.
- Maunsell, J. H., & Van Essen, D. C. (1983). Functional properties of neurons in middle temporal visual area of the macaque monkey. I. Selectivity for stimulus direction, speed, and orientation. *J Neurophysiol*, 49(5), 1127-1147.

Ratliff, F., & Riggs, L. A. (1950). Involuntary motions of the eye during monocular fixation. *J Exp Psychol*, 40(6), 687-701.

Salzman, C. D., Britten, K. H., & Newsome, W. T. (1990). Cortical microstimulation influences perceptual judgements of motion direction. *Nature*, 346(6280), 174-177.

Skavenski, A. A., Robinson, D. A., Steinman, R. M., & Timberlake, G. T. (1975). Miniature eye movements of fixation in rhesus monkey. *Vision Res*, 15(11), 1269-1273.

Zohary, E., Shadlen, M. N., & Newsome, W. T. (1994). Correlated neuronal discharge rate and its implications for psychophysical performance. *Nature*, 370(6485), 140-143.

Chapter 2: Responses to perceptually invisible image motion in extrastriate visual area MT in macaque monkeys

Abstract

Our eyes are constantly in motion. Even as we hold our gaze still, small eye movements jitter the image of the world on our retinae. It is known that these eye movements of fixation enable us to see normally by preventing the fading of a visual image due to adaptation of visual neurons. However, at the same time, they require the brain to convert a moving retinal image into a stable perception of the world. Little is understood about which brain areas respond during eye movements of fixation and how they are involved in achieving perceptual stabilization. Of the fixational eye movements that have been studied few have focused on drifts which are the slow movements occurring in between microsaccades. In order to gain insight into the process of visual stabilization we asked whether neurons in MT, a cortical area sensitive to visual motion, respond during drifts. We found that drifts elicit remarkably large responses in MT neurons due to the image motion they generate on the retina. Despite the fact that most neurons in our sample had preferred speeds much larger than the image speeds generated by drifts, almost all of them were modulated during drifts when these induced visual motion along the preferred direction of the neurons. Our results clearly show that neurons respond to drifts beyond early visual areas and that MT can specifically inform other areas about the direction of the small image motions induced by drifts. The signals provided by MT could then be used to eliminate global motion signals arising from eye movements during fixation.

Introduction

Our eyes move constantly and thereby create a retinal image of the world that is never still. Large, voluntary movements called saccades allow us to direct a particular part of an image onto our fovea, the area of the retina that is capable of the highest acuity visual processing. Much smaller eye movements occur during periods of fixation between saccades (Ditchburn & Ginsborg, 1953; Martinez-Conde, Macknik, & Hubel, 2004; Ratliff & Riggs, 1950). Based on their dynamics, the eye movements of fixation are categorized into three groups. Microsaccades are fast, jerk-like movements that are similar to saccades, but smaller in amplitude (Barlow, 1952; Hafed, Goffart, & Krauzlis, 2009; Steinman, Haddad, Skavenski, & Wyman, 1973; Zuber & Stark, 1965). They occur several times per second with a frequency that depends on the task at hand. Drifts are loosely defined as the slow movements occurring in between microsaccades (Adler & Fliegelman, 1934; Ratliff & Riggs, 1950; Skavenski, Robinson, Steinman, & Timberlake, 1975; Spauschus, Marsden, Halliday, Rosenberg, & Brown, 1999). Tremor consists of high-frequency low amplitude oscillations (30-100 Hz, depending on the study), superimposed on drifts (Adler & Fliegelman, 1934; Ditchburn & Ginsborg, 1953; Eizenman, Hallett, & Frecker, 1985; Ratliff & Riggs, 1950; Riggs, Armington, & Ratliff, 1954; Riggs & Ratliff, 1951; Spauschus et al., 1999).

We are unaware of our small eye movements made during fixation, but they play an important role in visual perception. Psychophysical evidence suggests that fixational eye movements prevent fading of images by constantly jittering the retinal locus of the image from a stationary object, precluding adaptation of neural responses to a static

visual scene (Ditchburn & Ginsborg, 1952). Fixation eye movements also appear to improve perception of fine spatial detail (Rucci, Iovin, Poletti, & Santini, 2007). Although the different types of fixational eye movements in concert seem to play an important part in visual perception, the role of each type of eye movement is unclear.

The eye movements of fixation also create a challenging problem for the brain: the ever-moving retinal image must be converted into perception of stability in the world. The brain meets this challenge flawlessly under normal circumstances, when we are unaware of the continuous image motion generated by the movements of our eyes. It seems likely that compensation for retinal image motion is an active process, because it can be made to fail under certain laboratory conditions, such as in the jitter illusion when we perceive the retinal image motion generated by our fixational eye movements (Murakami & Cavanagh, 1998). As a first step toward understanding how the brain stabilizes percepts in spite of motion of the retinal image, we must learn how the responses of neurons in visual areas are affected by the eye movements of fixation. If, for example, a motion area did not respond to the eye movements of fixation, we could conclude that the expected responses had been nulled at an earlier stage. If a motion area did respond to the eye movements of fixation, then we would obtain information about the representation of the resulting image motions to inform analysis of how the visual signals are nulled in downstream circuits.

In all visual brain areas that have been examined, neurons respond to retinal image motion generated by the eye movements of fixation. For example, the lateral geniculate nucleus, the primary visual cortex (V1), and extrastriate cortical area MT respond to the image motion caused by microsaccades (Bair & O'Keefe, 1998; Leopold

& Logothetis, 1998; Martinez-Conde, Macknik, & Hubel, 2000, 2002; Reppas, Usrey, & Reid, 2002). It seems plausible that the same mechanisms responsible for “saccadic suppression” could provide perceptual stability in spite of microsaccades (Brooks & Fuchs, 1975; Burr & Morrone, 2010; Burr, Morrone, & Ross, 1994; Campbell & Wurtz, 1978; Matin, Clymer, & Matin, 1972; Thiele, Henning, Kubischik, & Hoffmann, 2002). However, slow eye movements pose different problems, and perception does seem to be affected by the eye movements of smooth pursuit (Kerzel, Aivar, Ziegler, & Brenner, 2006; Schutz, Braun, Kerzel, & Gegenfurtner, 2008; Turano & Heidenreich, 1999; van Beers, Wolpert, & Haggard, 2001). In area V1 (Kagan, Gur, & Snodderly, 2008; Snodderly, Kagan, & Gur, 2001), a subset of neurons responds vigorously during fixation between microsaccades. To understand why these responses do not lead to perceptual instability, it is critical to analyze the image motions that drive the responses, determine whether responses to motion are transmitted beyond V1, and understand the representation of the image motions of fixation in the cortical motion pathways.

Extrastriate area MT provides a central representation of visual motion information that is critical for both perception (Newsome & Pare, 1988) and smooth pursuit eye movements (Newsome, Wurtz, Dursteler, & Mikami, 1985). Therefore, we decided to study the responses of MT neurons during the slow oscillations of eye velocity that occur during fixation and between microsaccades. Slow drifts drive firing rates when a visual stimulus is located in the receptive field of an MT neuron. The neural responses are direction selective, but do not depend on the speed preference of the neurons. Because MT responds to miniature deviations in image motion caused by drifts in eye velocity, the slow eye movements of fixation should engender percepts that the stationary world is

moving. We outline several mechanisms that could operate downstream from MT to keep the perception of a stationary, stable world.

Materials and Methods

Subjects

We recorded eye movements and neural responses from two adult male rhesus monkeys (*Macaca mulatta*, 7-13 kg). After initial training, monkeys were implanted with hardware to allow head restraint and scleral search coils to record eye movements, as described in detail elsewhere (Ramachandran & Lisberger, 2005). For one control experiment, we obtained eye movement data from both eyes of an additional male adult rhesus monkey who had bilateral scleral search coils. In an additional surgical procedure, we mounted titanium or cilux recording chambers (Crist instruments, Hagerstown, MD) over a 20 mm circular opening in the skull to allow access to MT for neural recordings.

For each experimental session, monkeys sat in a primate chair with their heads immobilized and received fluid rewards for accurately fixating or tracking visual targets presented on a screen in front of them. Experiments were conducted five times per week and lasted about 5 hours. All surgical and experimental procedures were approved in advance by the *Institutional Animal Care and Use Committee* of the University of California, San Francisco and were in strict compliance with the *NIH Guide for the Care and Use of Laboratory Animals*.

Visual stimuli

All experiments were conducted in a nearly dark room. Visual stimuli were presented on an analog oscilloscope (Hewlett Packard 1304A) with a refresh rate of 250 Hz. The oscilloscope was driven by 16-bit digital-to-analog converters on a digital signal

processing board in a PC. The display was positioned 20.5 cm from the monkey and subtended a 67° horizontal by 54° vertical visual angle.

First we mapped the receptive field of the neurons we were recording from while the monkey was required to maintain fixation within one degree of a bright spot which was presented at the center of the screen. After manually locating the receptive field, the direction and speed tuning of each neuron was measured by placing a patch of random dots in the receptive field of the neuron. Patches matched the size of the receptive fields of the neurons we recorded from and were either $5^\circ \times 5^\circ$ with 50 dots, or $8^\circ \times 8^\circ$ large with 128 dots placed at random locations within their aperture. During each stimulus presentation dots moved coherently in a given direction at a given speed for 300 ms and vanished for 200 ms before reappearing at the same location, but moving either at a different speed (speed tuning) or in a different direction (direction tuning). For each mapping trial either 5 randomly interleaved directions or speeds were presented before the monkey received a reward for maintaining proper fixation.

All data reported in this paper came from the fixation portion at the beginning of a pursuit task. These trials began when a $0.3 \times 0.3^\circ$ square appeared in the center of the screen as the fixation target. The change in fixation target cued the monkey that the task had changed. Following an arbitrary time between 500-900 ms a $5 \times 5^\circ$ or $8 \times 8^\circ$ patch of random dots appeared in the receptive field of the neuron for a randomized time between 300-900 ms. The random dot patch was the same as the one we used for mapping, however in this segment the dots were stationary. This fixation segment with a static patch in the receptive field was used for computing the spike-triggered averages and Fourier transforms of firing rates and eye movements. In these analyses data was aligned

to the onset of the patch. After the interval containing the static patch, the dots began moving coherently within the fixed aperture of the patch for 100 ms and the fixation target disappeared at the same time, cueing the monkey to pursue the patch. This segment was used to study the effects of fixational eye movements on neural responses at the onset of a motion stimulus. For this purpose, data were aligned to the beginning of stimulus motion. Even though the monkey had been cued to pursue the motion target, the monkey did not yet initiate pursuit during this segment because of the delay between motion and pursuit onset, which enabled us to study the effects of fixational eye movements. Presenting the stationary dots before introducing motion allowed us to separate the MT response to the onset of a visual motion from the response to the onset of light in the receptive field. Typically, 4-6 target motions, each consisting of different stimulus speeds or directions, were randomly interleaved. Subjects usually completed 2000-3600 pursuit trials in each daily experiment. For all analyses, trials were included only if the subject maintained fixation within 1 degree of the fixation point and no microsaccade occurred.

MT recording

We recorded 104 neurons in visual area MT in three hemispheres of two monkeys (52 neurons from left and right hemispheres in monkey Y, 52 neurons from right only in monkey J). We used a Thomas microdrive (Thomas Mini-Matrix 05, Thomas Recording, Giessen, Germany) to lower quartz-shielded tungsten electrodes vertically into MT with impedances from 1 to 4 M Ω . MT was identified based on stereotaxic coordinates, directional and speed response properties of neurons, receptive field sizes, retinotopic organization, and surrounding cortical areas (Maunsell & Van Essen, 1983). We typically

recorded from neurons with receptive field centers within the central 5° of the visual field.

Electrical signals were amplified and digitized for on-line spike sorting and spikes were initially assigned to single neurons by using a template matching algorithm (Plexon MAP, Plexon Inc., Dallas, TX). After the experiment we used a combination of visual inspection of waveforms, projections onto principal components, template matching, and refractory period violations in Offline Sorter (Plexon Inc, Dallas, TX) to sort and assign spikes to well isolated single units. After sorting, waveforms were converted to timestamps with 1 ms precision for analysis. Firing rates were obtained by convolving spikes trains with a Gaussian window (SD 10ms).

To obtain the tuning properties of each cell, we fit speed and direction tuning curves with Gaussian functions:

$$R(s) = R_0 + a * \exp \left\{ - \left[\frac{\log\left(\frac{s}{ps}\right)}{c + d * \log\left(\frac{s}{ps}\right)} \right]^2 \right\}$$

$$R(\theta) = R_0 + A * \exp \left\{ - \frac{1}{2} \left[\frac{\theta - pd}{C} \right]^2 \right\}$$

(s – speed, θ – direction, R_0 – baseline firing rate, a – amplitude of speed tuning curve, A – amplitude of direction tuning curve, ps – preferred speed, pd – preferred direction, c – width of speed tuning curve, C – width of direction tuning curve, and d – skew parameter of speed tuning curve). The angle $\theta - pd$ was restricted to $[-\pi, \pi]$ degrees.

Behavioral data

Eye position and velocity signals were sampled and stored at 1000 Hz. Velocity signals were obtained by passing eye position signals through an analog differentiator. The circuit differentiated frequency content from 0 to 25 Hz and filtered higher frequencies with a roll-off of 20 dB/decade. Before analysis, each trial record was inspected and rejected if a saccade or microsaccade occurred within the time window chosen for analysis (epoch without patch: 350 ms, static patch: 600 ms, dynamic patch: 200 ms). For analyses of Fourier and principle components, as well as spike-triggered averages, we excluded the first 130 ms after the onset of the random dot patch in order to ignore spikes that were triggered by the onset of a visual stimulus rather than eye movements. For each target motion, we counted the number of spikes across trials 130-600 ms after stimulus onset and included the data set if we had a total of at least 200 spikes per cell.

To test whether the oscillations in eye velocity occurred along a given direction, we determined the principle components of velocity for each experiment. Principle components analysis can tell us two things: (1) the first principle component tells us the direction along which most variance in eye velocity occurs. This direction was consistent whether we used raw data, or digitally filtered data with a low-pass (< 25 Hz), or band-pass filter (3-7 Hz). (2) The magnitude of the two Eigen values tells us how strongly eye velocity is modulated along each principle component. If the Eigen values are equal in magnitude, the eye velocities are isotropic, whereas if one value is much higher, the eyes move mainly along one direction. We report the degree of isotropy in terms of the ratio of the first and the second principle component (PC1/PC2).

Fourier transforms were computed on traces that were first multiplied with a symmetric Henning filter and then zero padded. The Fourier transform was calculated for each trial and then averaged for each experiment.

Spike-triggered averaging

We calculated the spike-triggered averages (STAs) of image velocity and position which were generated by eye movements during fixation. This allowed us to look at the average movement surrounding a spike of a given neuron:

$$STA(\tau) = \frac{1}{N} \sum_{i=1}^N image(t_i - \tau)$$

Where $image(t)$ stands for either image velocity or position, t_i is the time of occurrence of a spike, τ is the temporal lag between the spike and movement parameter, and N is the total number of spikes (Dayan, 2001). The amplitude of the STA of velocity was calculated as the peak minus the trough occurring before the spike.

Results

The smooth eye movements of fixation

During epochs of fixation between microsaccades, monkeys show smooth drifts in eye movements that appear as oscillations in the eye velocity traces. In figure 2.1 (left panel), for example, the horizontal and vertical eye velocity in a single trial showed oscillations with a period of about 300 ms and additional fluctuations at higher frequencies. The peak-to-peak amplitudes of the oscillations in eye velocity were less than 2 deg/s, and were somewhat larger in vertical versus horizontal eye velocity in this example.

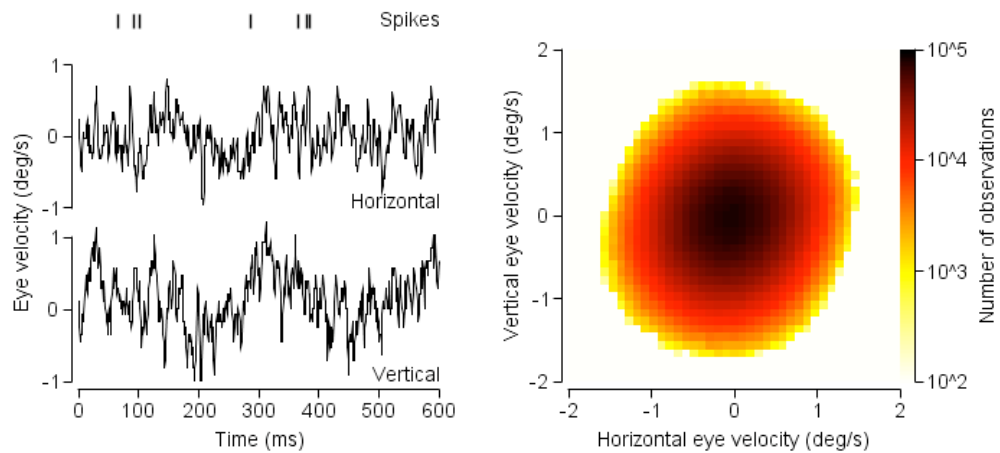


Figure 2.1

Left panel: Eye velocity traces and spikes for one example trial during 600ms of fixation.

Top row: spikes are represented by vertical lines at the time of occurrence. Middle and

bottom row: horizontal and vertical eye velocity as a function of time. Trials are aligned to

the onset of a stationary random dot patch in the receptive field of the neuron. Right panel: Two-dimensional histogram of eye velocity during fixation for all experiments for monkey Y.

The distribution of smooth eye velocities during fixation was centered near zero with the overwhelming majority of the observations falling between -0.75 and $+0.75$ deg/s. In figure 2.1 (right panel), each pixel shows the number of observations of a given pair of horizontal and vertical eye velocities. We sampled eye velocity in 1 ms steps in the intervals between microsaccades in each trial across all experiments in our dataset, and then combined all observations into a single distribution. The distribution deviates slightly from circular and is biased in the first and third quadrants, indicating a slight tendency for the smooth eye velocities of fixation to be right and up, or left and down.

Principle component analysis confirmed the slight directional bias in the smooth eye velocities of fixation and showed that it was present in almost all experimental sessions. In figure 2.2, each symbol shows data from a different experimental session and represents the end of a vector, where the direction of the vector shows the direction of the first principle component and the length of the vector indicates the amplitude ratio of the second/first principle component. Most of the symbols plot in the up-right quadrant, indicating a uniform direction of the first principle component along the up-right/down-left axis. Most plotted at an amplitude of approximately 2, indicating that the first principle component was twice as large as the second. Averaging across all experimental sessions separately for the two monkeys revealed that the direction of the first principle component was 26 and 49 deg for monkey Y and J. The amplitude ratio averaged 2.0 and

1.75 in monkeys Y and J. The quantitative findings in figure 2.2 were virtually unchanged when we filtered the eye velocity traces to remove higher frequencies (both for 25 Hz low pass and 3-7 Hz band pass).

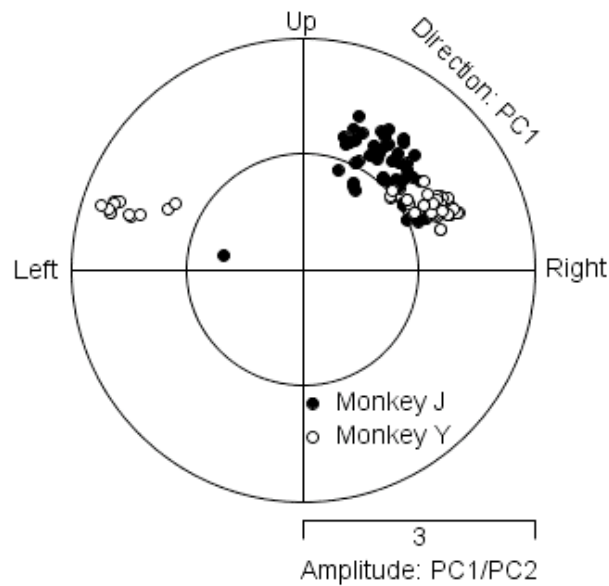


Figure 2.2.

Direction of eye velocity during epochs of drifts. Each point represents data from one experiment. Direction was determined by the direction of the principle component that explained most variance in eye velocity. The distance of each point to the center of the plot describes the ratio of variance explained by the first and second principle components (PC1/PC2).

Responses of MT neurons during the smooth eye movements of fixation

Our behavioral task was designed to study the responses of MT neurons under 3 conditions that differed in the nature of the visual stimulus. The task began with an interval when the monkey was required to fixate a spot target on an otherwise dark screen (Figure 2.3, left panel). In most neurons, firing rate is low during fixation with a dark background because of the lack of visual stimulation in the receptive field. In the next interval, the monkey continued to fixate but a patch of static random dots appeared in the receptive field (Figure 2.3, center panel). The onset of the visual stimulus in the receptive field of the neuron caused a strong transient response in most neurons, followed by firing at a slightly higher rate than with a dark background. In the final interval, the dots within the patch moved coherently in a given direction at a specified speed. MT neurons responded to the motion with a large transient change in firing rate followed by an elevated sustained response. In our analysis, we take advantage of the specifics of the three stimulus conditions to understand when and how the smooth eye velocities duration fixation affect neural responses in visual area MT.

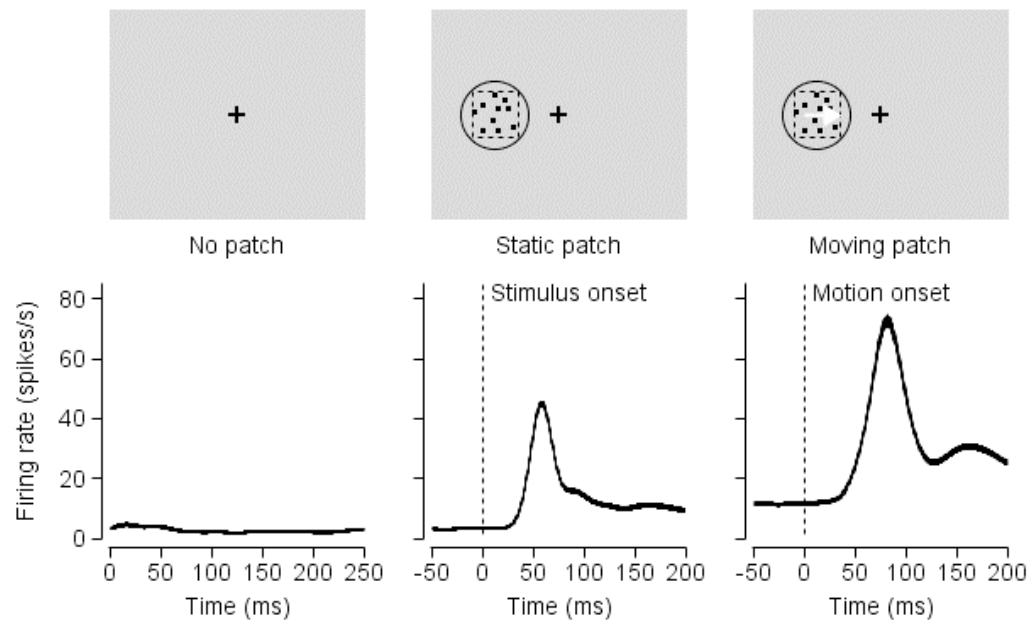


Figure 2.3.

Example MT response during the three different epochs of fixation. The top row shows the visual stimulus during each interval and the bottom row the average MT response for one neuron. Left column: A fixation point was presented at the center of the screen for a random time between 500-900ms. During this time the monkey initiated fixation. Middle column: A patch of static random dots appeared in the receptive field (circle) of the neuron for a random time between 300-900ms. Right column: The dots started moving in one of several directions and speeds for 100ms.

Fourier analysis of the eye velocity between microsaccades revealed oscillations at low frequencies around 4-5 Hz (Figure 2.4). The amplitude of the oscillations was approximately 0.2 deg/s for horizontal and vertical eye velocity in both monkeys. Many neurons showed corresponding modulations in firing rates at the same low frequencies.

The Fourier transforms were calculated on responses collected during fixation of the static patch, during which the only source of retinal image velocity were drifts in eye movements. Because MT neurons are known to respond to visual motion in their receptive field it is likely that the modulation in firing rates is caused by the small oscillations in image velocity, an issue we will address below.

Eye velocity contained further peaks at higher frequencies which were not present in neural responses. The additional peak in eye velocity was centered around 15 Hz and was most pronounced for horizontal eye speed in monkey Y. However, neural responses were not modulated at this frequency. Because the eye signals were passed through an analog filter, high frequency tremor is suppressed in our eye velocity traces. In contrast to the behavioral signal, spike trains were unfiltered and recorded at a resolution of 1000 Hz. Therefore spike trains could contain high frequency modulations which would appear in the Fourier transforms if these were present. However, whether we looked at the frequency content of firing rates or spike trains, no significant modulation at higher frequencies appeared and neural responses decayed rapidly with increasing frequencies. This suggests that high frequency movements contribute little to the overall power in the neural response during the time intervals and stimulus conditions we inspected.

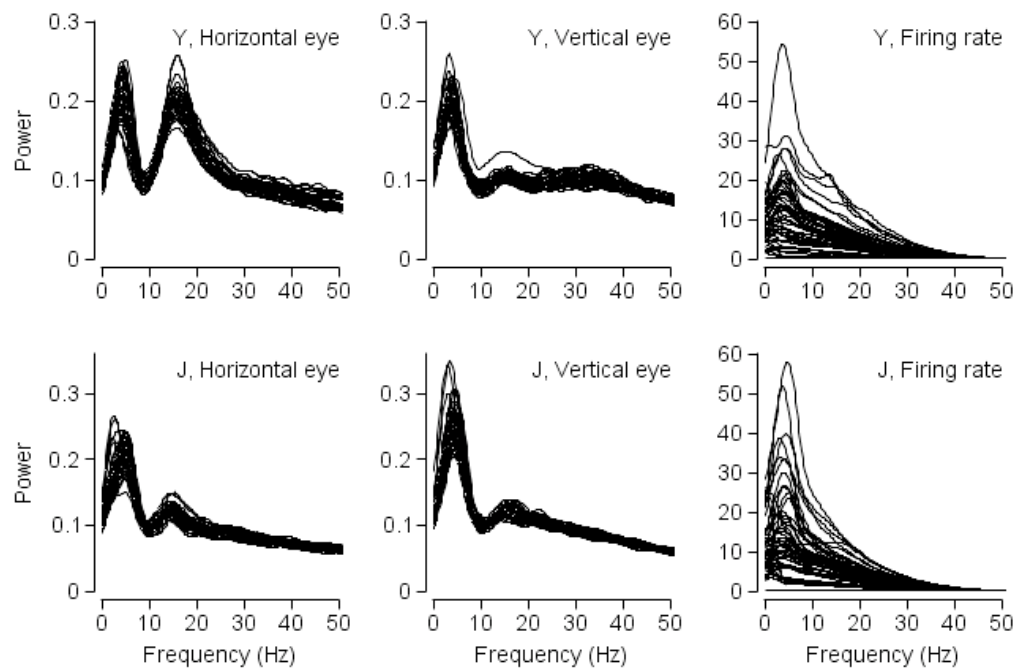


Figure 2.4.

Frequency content of eye velocity and MT responses during fixation. The Fourier transform of horizontal and vertical eye velocity, as well as MT firing rates is shown for data recorded during fixation of the static patch. Each black trace corresponds to one experiment. Top row shows data for monkey Y, bottom row for monkey J.

In one monkey equipped with binocular scleral search coils, we verified that the low frequency oscillation at 4-5 Hz was positively correlated between the two eyes. The black traces in figure 2.5 show the autocorrelation in horizontal (Figure 2.5A) and vertical (Figure 2.5B) eye velocity for both eyes. The negative troughs surrounding the peak in the autocorrelation again revealed the low frequency oscillation which appeared in the Fourier transforms. This oscillation appeared in the cross-correlation of horizontal

and vertical eye velocity between both eyes (red trace) as well with the same sign and following the same time course as in the autocorrelation. The peak of the cross-correlation between both eyes had a value of 0.70 and 0.69 for horizontal and vertical eye velocity. The positive peak in the cross-correlation at zero lag together with the fact that the cross-correlation followed the same slow oscillation as the autocorrelation with equal sign demonstrates that the low frequency oscillations arise from conjugate rather than vergence eye movements.

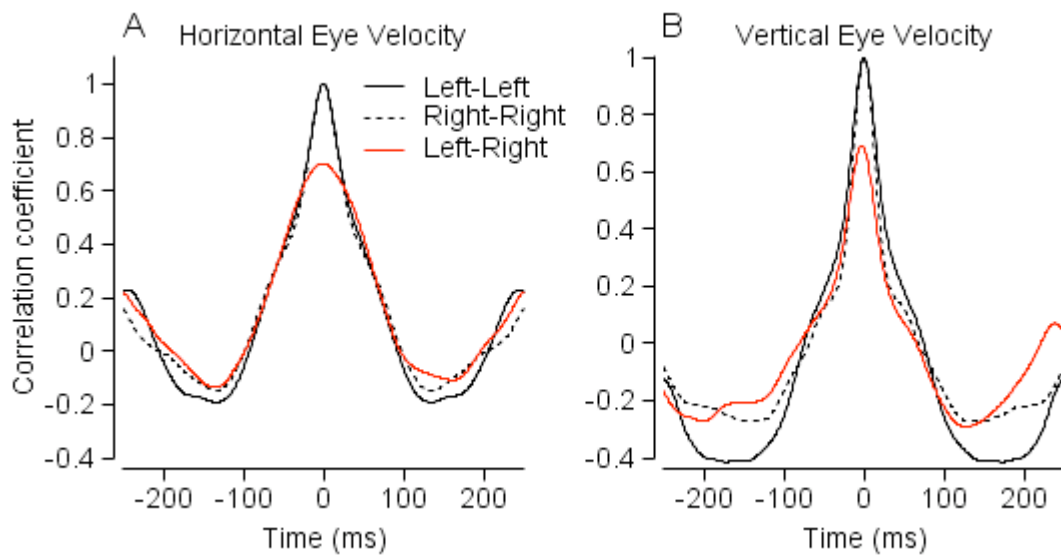


Figure 2.5.

Cross-correlation of horizontal (A) and vertical (B) eye velocity between both eyes. Left-Left and Right-Right refer to the autocorrelation of eye velocity of the left and right eye. Left-Right is the cross-correlation between the left and right eye.

Spike-triggered averages (STAs) provided direct evidence that MT neurons respond to the small fluctuations in image velocity caused by the eye movements of fixation. The STA describes the image velocity that on average surrounds each spike. Because MT neurons respond preferentially to motion along a preferred axis (Albright, 1984; Lisberger & Movshon, 1999; Maunsell & Van Essen, 1983; Rodman & Albright, 1987; Snowden, Treue, & Andersen, 1992), we separated image velocity into components parallel and orthogonal to the preferred direction of each cell.

Figure 2.6 shows that spikes were consistently preceded by a positive deviation in image velocity of about 0.2 deg/s in the preferred direction of cells (Figure 2.6, left column). The shape of the STAs demonstrates again that the drifts in eye velocity are oscillatory in nature. Indeed, reliably across experiments and monkeys the STAs have multiple positive and negative peaks. Subsequent positive or negative peaks are separated by about 200 ms, which corresponds to an oscillation with a frequency of 5 Hz, consistent with the findings of the frequency analysis in figure 2.4. The eye velocity orthogonal to the preferred direction did not contain clear structure (Figure 2.5, right column).

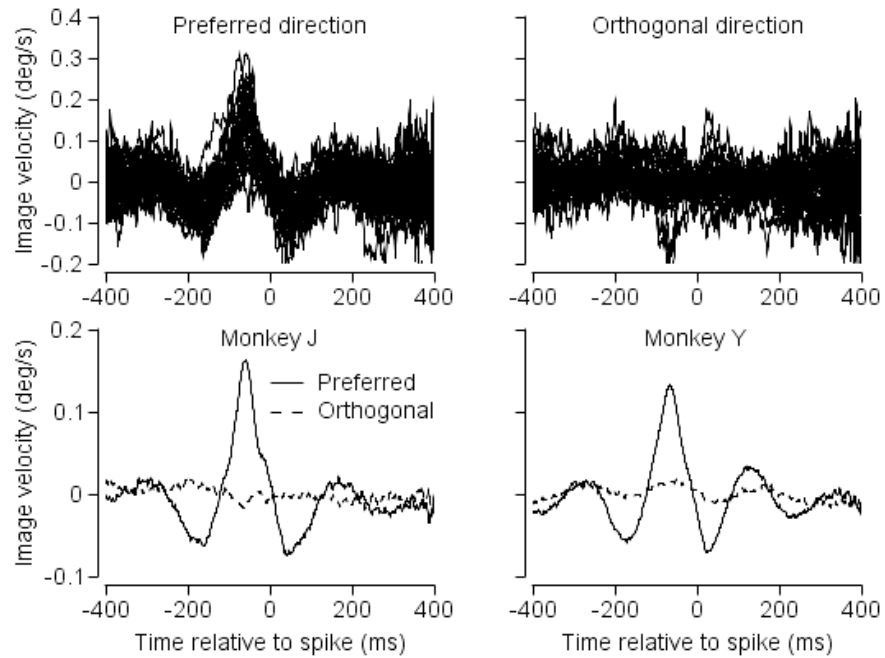


Figure 2.6.

Spike-triggered averages of image velocity during fixation of the static patch. Top row: Each trace is the spike-triggered average for one neuron for monkey Y. Zero marks the time of spike occurrence. The STAs were calculated separately for image velocity in and orthogonal to the preferred direction of each cell. Bottom row: The average STA across neurons is shown for both directions and both monkeys.

The latency between image velocity and spike occurrence suggests that the eye movements drive the MT response rather than the other way around. The latency as indicated by the peak of the STA is 58 and 67 ms for monkey Y and J. This is in the realm of visual latencies of MT neurons, especially considering that latencies of MT

responses are longer for slow speeds (Lisberger & Movshon, 1999). Normalizing the STAs to reveal the cross correlation between image velocity and spikes, showed that the peak correlation coefficients between image velocity and spikes are 0.23 and 0.21 for monkey Y and J. Therefore, taking into account the latency of the neural response, image velocity and therefore eye movements account for approximately 4% of the variance in MT firing rates during fixation.

All neurons responded to small fluctuations in image velocity, independent of their tuning properties. Even though MT neurons are tuned for the speeds of faster target motions (Lagae, Raiguel, & Orban, 1993; Lisberger & Movshon, 1999; Maunsell & Van Essen, 1983; Rodman & Albright, 1987), the amplitude of the STAs did not depend on the preferred speeds of the neurons (Figure 2.7). This means that virtually all MT cells, no matter whether their preferred speed was 1 or 40 deg/s, responded to the image velocity generated by drifts in the eye movements of fixation. It is important to note, however, that the amplitude of the STA is limited by the amplitude of the drifts.

The sensitivity of the neurons to drifts was further independent of the shape of the speed tuning curves (Figure 2.7). Most cells in our sample had Gaussian shaped tuning curves (tuned cells) with low firing rates for slow speeds and only one fifth of the tuning curves resembling low pass filters (Lagae et al., 1993; Orban, Kennedy, & Bullier, 1986; Orban, Kennedy, & Maes, 1981). Because low pass cells respond well to stimuli with small speeds, one might expect to observe larger STA amplitudes in these cells. However, the STA amplitudes were independent of the shape of the tuning curves in addition to being independent of the preferred speed of cells. Even tuned cells which have low firing rates for the image velocities caused by drifts had significant STA

amplitudes for image velocity in the preferred direction, but not orthogonal to it. Therefore, even when firing rates are low as was the case for most of our cells during drifts, the spikes that are generated contain information about direction of motion.

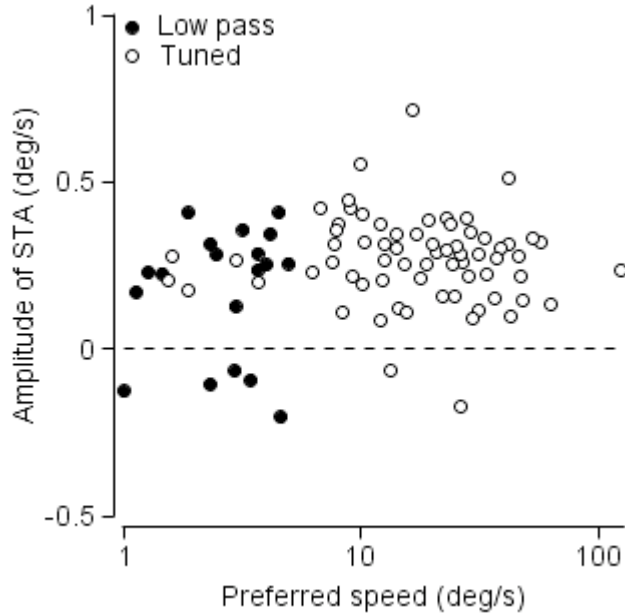


Figure 2.7.

The amplitudes of STAs are independent of the preferred speeds of the neurons. For each cell we plotted the amplitude of the spike-triggered average of image speed along the preferred direction as a function of preferred speed.

Analysis of the image speeds and firing rates during fixation revealed a consistent relationship between the fluctuations in retinal image speed and the modulations in firing rates during fixation (Figure 2.8, left panel), even before the stimulus moved. To perform

this analysis, we combined the data across neurons and grouped trials according to the image velocity generated by fixation eye movements in the 50 ms time interval from 200 to 250 ms after the appearance of a stationary visual stimulus. We then averaged the eye velocity and firing rate within each group to obtain the families of traces that appear in Figure 2.8A and C. As expected, given how the traces were grouped, the eye velocity for the difference groups peaks at different values 225 ms after the appearance of the visual stimulus. The firing rates peak about 60 ms later, consistent with the latencies found in the STAs. The values of the peaks in firing rate varied across groups, in the same sequence as the peaks in image velocity. Modulations were larger for image motion in the preferred versus null direction, and the peak/trough of firing rate varied from 5 to 35 spikes/s as the image velocity varied from -0.6 to 0.7 deg/s.

The smooth eye movements of fixation also affected the responses of MT neurons to the onset of target motion (Figure 2.8B and D). To perform this analysis, we again grouped trials according to the image velocity, now in the 50 ms interval from 25 ms before to 25 ms after the onset of target motion, and averaged the eye velocity and firing rate within each group. Comparison of the firing rates across groups revealed that the latency of MT responses was delayed in relation to the image velocity present at the time the target started to move, with null-direction image motion causing increases in response latency. In contrast, the peak of the firing rate response of MT neurons was largely unaffected by small deviations in image velocity due to the eye movements.

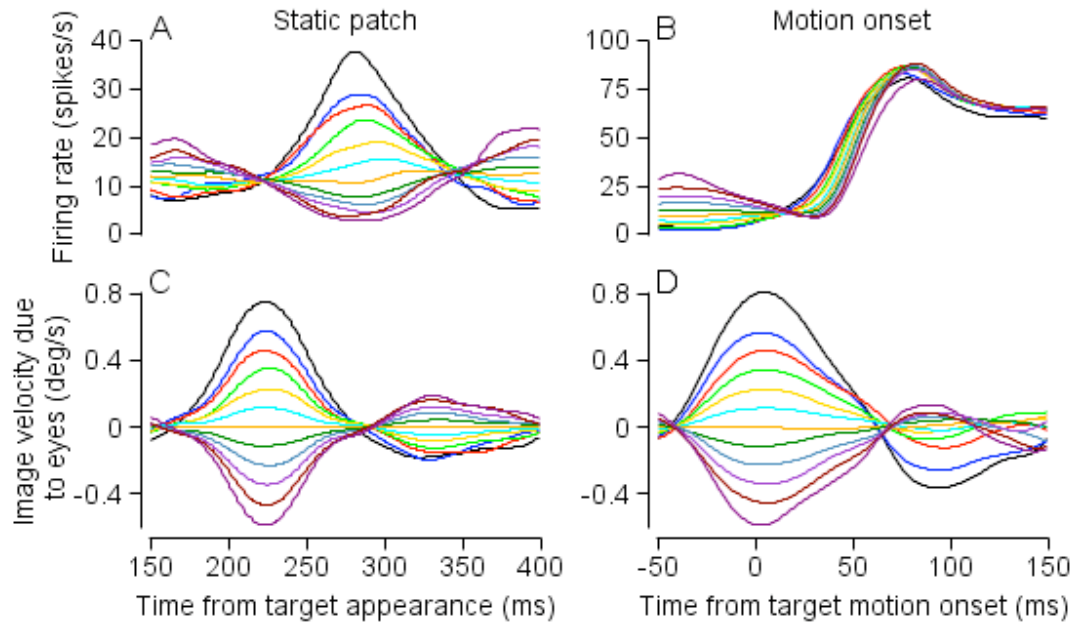


Figure 2.8.

Image velocity generated by drifts modulates firing rates in MT neurons. A and C, neural and behavioral responses during fixation of the static patch. Trials were grouped according to deviations in image velocity 200-250 ms after patch onset. We only considered image velocity in the preferred direction of cells. For each group, trials were averaged across experiments and monkeys. C, average image velocity for each group. A, average firing rate for the same groups as in C. B and D, same analysis as in C and D except trials were aligned to motion onset in the patch at 0 ms (see figure 2.3, right panel) and were grouped by deviations in image velocity due to eye movements -25 to 25 ms around motion onset. Image velocity in D does not include stimulus velocity. Experiments were included in which the stimulus moved within 90 degrees of the preferred direction of the neurons.

The firing rate modulations that we observed during the eye movements of fixation are caused by the visual motion signals generated by the eye movements, not by extra-retinal inputs. In figure 2.9, we have subtracted the firing rates for the group with the smallest absolute image motions from the firing rates for each other group, and then plotted the peak firing rate of each group as a function of the peak image velocity. For analysis of the intervals shown in figure 2.8A, there was a strong relationship between the evoked firing rate and image velocity when the visual stimulus was stationary in the receptive field of the neuron under study (Figure 2.9A, open circles). In contrast, the relationship was much shallower, and barely present, if we conducted the same analysis on an interval with a fixation point but without a stationary stimulus in the receptive field of the neuron (Figure 2.9A, open triangles). While this residual modulation could potentially reflect extra-retinal inputs to MT, it is likely caused by weak visual stimulation in the receptive field. We conducted our experiments in dim light and therefore faint reflections of objects in the room generated a weak visual stimulus on the screen. A further reason for weak modulations might be the sampling of our MT neurons. We recorded from parafoveal MT where many neurons have receptive fields adjacent to or slightly overlapping with the bright spot that served as the fixation point. As with the reflections, the single spot can provide a suboptimal motion stimulus during eye movements that can elicit weak neural responses.

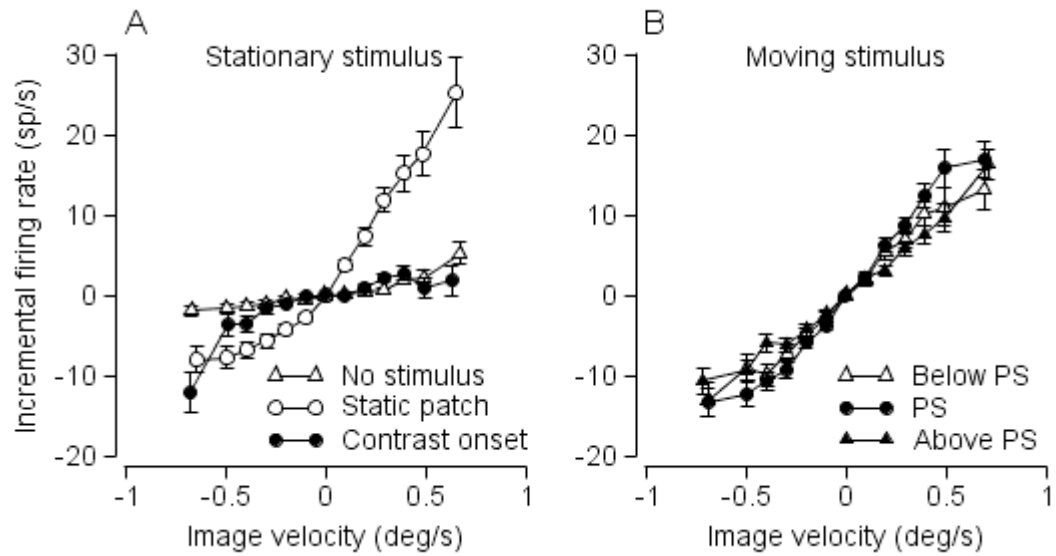


Figure 2.9.

Neural responses are substantially modulated by image velocity. Incremental firing rates are plotted against image velocity for the groups shown in figure 2.8. A, Firing rates are shown for the three different stimulus conditions described in figure 2.3: no stimulus in the receptive field (RF), sustained response with static patch in the RF, and peak transient response to the onset of the static patch (labeled contrast onset). For each group we averaged trials across experiments and monkeys. Error bars indicate standard errors of the mean. B, Incremental firing rates at the onset of the transient response to motion. We averaged experiments depending on whether the dots moved below, at, or above preferred speed (PS) of the neurons.

The image velocity at the time of appearance of a stationary stimulus also had only a weak effect on the peak of the transient firing rate caused by the appearance of a stationary stimulus (Figure 2.9A, filled circles). This is likely due to the fact that the

onset of luminance provides a strong visual stimulus during which the neurons are insensitive to small deviations in retinal speed.

Figure 2.9B shows that the effect of image motion during fixation on responses to subsequent stimulus motion cannot be attributed simply to effects of eye velocity drifts on the image speed at the onset of the image motion. Even though figure 2.8B indicates that the eye movements of fixation appear to affect the latency of the neural transients, differences in latencies result in differences in magnitude at each time during the initial firing rate response. The effect of image motion due to the eyes on firing rates 45 ms after motion onset are strong, but do not depend on whether the speed of the stimulus was above or below the preferred speed of the neuron. This observation is important because we would expect a direct effect of small eye movements on the magnitude of image motion to cause the relationships in figure 2.9B to have a positive versus negative slope depending on whether image speed is on the rising or falling arm of the neuron's tuning curve.

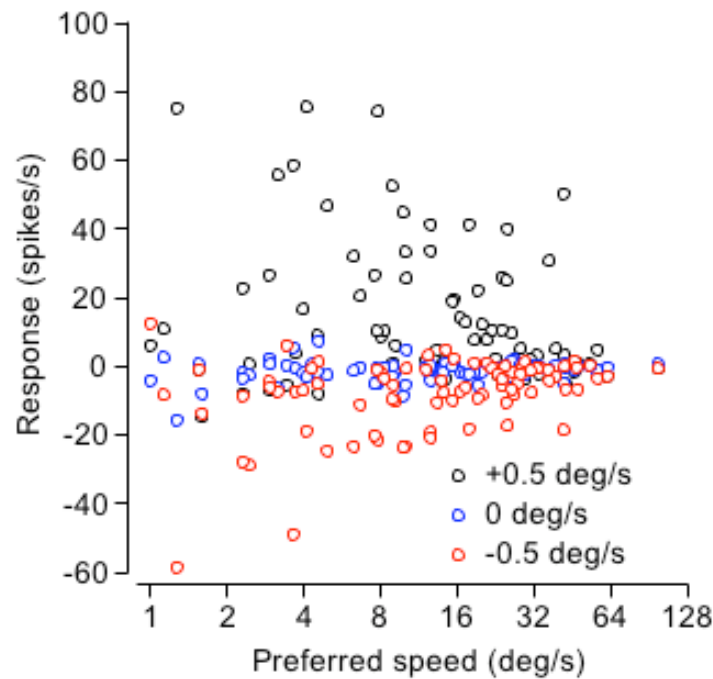


Figure 2.10.

Population response to drifts. Firing rates relative to mean firing rate are plotted against preferred speed for each cell. Black dots show responses to image velocity of 0.5 deg/s, blue dots responses to 0 deg/s, red dots to image velocity of -0.5 deg/s.

To understand why the smooth eye movements of fixation cause orderly responses in MT neurons but are not seen perceptually, we will need to document the population response in area MT during the smooth eye movements of fixation. To do so, we have repeated the grouping analysis, but now analyzing each neuron separately. For each neuron, we have averaged the eye velocity and firing rate for groups of trials in which the image speed 200 to 250 ms after the onset of the stationary stimulus was within 0.1 deg/s of -0.5, 0, of +0.5 deg/s. Then we measured the peak firing rate approximately

60 ms later, and plotted 3 symbols for each neuron showing the firing rate response as a function of the neuron's preferred speed. For image speeds of about -0.5 or $+0.5$ deg/s (Figure 2.10, black versus red symbols), the firing rates were almost uniformly higher or lower than for image speeds of 0 deg/s (blue symbols). Importantly, the population response did not show a clear peak at any preferred speed, as it would have for image motion created by faster stimulus motions. Thus, the population response to the smooth eye movements of fixation appears to signal the direction, but scantily the speed of image motion.

Discussion

We found that drifts in fixation eye movements elicit responses in single neurons in visual area MT. During drifts eyes usually move slower than 0.75 deg/s and despite these small amplitudes, responses to drifts were found in almost all neurons in our sample, independent of their preferred speeds or the shape of their tuning curves. This is unlike findings in V1 where neurons responding to drifts generally have low preferred speeds (Kagan et al., 2008). MT neurons responded only when drifts generated image velocity in their preferred direction. The size of the neural modulation was remarkably large: across the population a difference in image velocity of just over 1 deg/s generated an average difference in firing rate of over 30 Hz. Finally, we showed that the majority of the modulation in the neural response is due to the visual motion generated by eye movements rather than extra-retinal signals due to corollary discharge.

Our results demonstrate that drifts generate sufficient image velocity to elicit neural responses in the visual pathway. Drifts might thereby play an important role in preventing adaptation of neurons when we hold our gaze still on a static visual scene (Steinman et al., 1973). Microsaccades might certainly contribute to the maintenance of vision as well and could be necessary for the maintenance of eccentric vision where it is possible that drifts are too small to generate responses in larger receptive fields. Most likely drifts and microsaccades act in concert to maintain vision (Ditchburn & Ginsborg, 1952; Gerrits & Vendrik, 1974; Martinez-Conde et al., 2004; Riggs, Ratliff, Cornsweet, & Cornsweet, 1953; Rucci & Desbordes, 2003). Visual fading occurs as fast as 80 ms and therefore drifts could be crucial for enabling vision during time periods where we make

few microsaccades (Coppola & Purves, 1996). This happens, for example, during high-acuity tasks such as threading a needle, where the frequency of microsaccades decreases to approximately 0.4 (Bridgeman and Palca, 1980, Ko et al., 2010). In addition to preventing perceptual fading, fixational eye movements have been implicated in other functions, for example improving discrimination of fine spatial detail (Rucci et al., 2007). It remains to be seen how drifts in particular contribute to any of these functions.

Irrespective of the possible contributions of fixational eye movements to visual perception, the constant motion of the eyes during fixation creates a challenging problem for the brain. The visual system must convert a continuously moving retinal image into a stable perception of the outside world. One possibility is that the brain first estimates the image velocity caused by eye movements of fixation and then subtracts it from the observed retinal velocities. In principle, there are two ways to estimate the image velocity caused by eye movements. First, the brain could rely on an estimate of eye velocity to extract the resulting image velocities. If eye movements are generated centrally, as was shown for microsaccades (Hafed et al., 2009), this could be achieved through an efference copy signal. Second, image velocity could be estimated directly from visual signals by extracting the global motion affecting all points of the image. In fact, the jitter illusion provides evidence that the stabilization of the retinal image relies on visual rather than extra-retinal signals (Murakami & Cavanagh, 1998). In order for this model to work, the brain must precisely estimate the magnitude and direction of motion due to all fixational eye movements, even for the miniature drifts during fixation. Our data shows that the population of MT neurons is capable of estimating the direction of motion despite

the very low retinal speeds involved and thereby might play a crucial role in providing the appropriate signal for stabilizing our visual perception.

Another way to eliminate image motion caused by eye movements could rely on center-surround antagonism found in many visual neurons. In the salamander retina, for example, cells have been found that are excited by a motion stimulus in the center of the receptive field but are completely silent when the coherent stimulus extends to the surround (Olveczky, Baccus, & Meister, 2003). In MT, about half of the neurons have large antagonistic surrounds (Allman, Miezin, & McGuinness, 1985a, 1985b; Born, 2000; Raiguel, Van Hulle, Xiao, Marcar, & Orban, 1995; Tanaka et al., 1986). Global motion provides coherent motion across the entire visual field, stimulating both the center and surround of neurons simultaneously. This might cause potential neural responses to be canceled out by the antagonistic relationship between the center and surround. For these neurons, it remains to be seen whether global motion due to fixational eye movements elicits any response. In our study we presented small stimuli in the center of the receptive fields of MT neurons, thereby excluding surround effects. However, at least for humans, when we look at the fixation point and the static patch appears on the screen, it does not jitter. Thus another mechanism, aside from the inhibitory surround must be involved in eliminating visual motion signals due to drifts. Even if in the antagonistic subpopulation global motion signals are eliminated during normal vision, the rest of MT might still be affected by fixational eye movements and these responses would have to be compensated for at a later stage.

In a Bayesian framework stabilization of vision due to fixational eye movements could be obtained by a simple mechanism that has previously been proposed for

explaining perceptual phenomena. Perception as well as smooth pursuit eye movements have a bias towards underestimating the speed of low-contrast stimuli (Lisberger & Westbrook, 1985; Spering, Kerzel, Braun, Hawken, & Gegenfurtner, 2005; Stone & Thompson, 1992; Thompson, 1982; Tychsen & Lisberger, 1986). Various studies have been able to explain these observations assuming that the brain has a prior towards zero speed (Hurlimann, Kiper, & Carandini, 2002; Stocker & Simoncelli, 2006; Weiss, Simoncelli, & Adelson, 2002). Applying a prior towards zero speed downstream from MT could diminish the readout of motion signals to such a degree that we interpret the very low speeds generated by drifts as stationary.

Whatever the mechanism for stabilizing the retinal signals due to fixation eye movements, it appears to occur at or after the level of MT. Indeed, we show that at least a subpopulation of neurons does respond to drifts. This observation is in contrast to conclusions of previous studies which have suggested that the effects of eye movements are removed from the visual signals before they reach MT (Pitkow, Sompolinsky, & Meister, 2007; Sasaki, Murakami, Cavanagh, & Tootell, 2002).

The fact that MT neurons respond to drifts could have an impact on various neural response properties, such as the magnitude and variance of firing rates as well as neuron-neuron correlations. During fixation of a stationary stimulus the increase in firing rate for image velocity along the preferred direction is larger than the decrease in firing rate caused by image velocity in the non-preferred direction, likely resulting in a net increase in firing rate because of drifts. Further, the variance of neurons in MT is known to be weakly correlated. During fixation of a stationary stimulus, a portion of that correlation is likely to arise from the common visual signal generated by drifts and it remains to be

seen how large that contribution is. Future studies can elucidate the impact of drifts by comparing neural responses to stimuli with and without retinal image stabilization and can avoid contamination by drifts by stabilizing a stimulus on the retina when this is needed. Finally, it is unknown whether drifts affect steady-state responses during fixation of dynamic stimuli, the circumstances under which MT is most commonly studied in laboratories.

Despite the fact that MT is rarely studied in the context of stationary stimuli, this situation is most similar to holding our gaze still during natural vision of static scenes. This is an action we repeat many times over the course of an hour or even minutes. Knowing that MT carries visual signals in these situations might therefore be an important piece to understanding the achievement of normal vision.

References

- Adler, F. A., & Fliegelman, M. (1934). Influence of fixation on the visual acuity. *Arch Ophthalmol*, 12, 475-483.
- Albright, T. D. (1984). Direction and orientation selectivity of neurons in visual area MT of the macaque. *J Neurophysiol*, 52(6), 1106-1130.
- Allman, J., Miezin, F., & McGuinness, E. (1985a). Direction- and velocity-specific responses from beyond the classical receptive field in the middle temporal visual area (MT). *Perception*, 14(2), 105-126.
- Allman, J., Miezin, F., & McGuinness, E. (1985b). Stimulus specific responses from beyond the classical receptive field: neurophysiological mechanisms for local-global comparisons in visual neurons. *Annu Rev Neurosci*, 8, 407-430.
- Bair, W., & O'Keefe, L. P. (1998). The influence of fixational eye movements on the response of neurons in area MT of the macaque. *Vis Neurosci*, 15(4), 779-786.
- Barlow, H. B. (1952). Eye movements during fixation. *J Physiol*, 116(3), 290-306.
- Born, R. T. (2000). Center-surround interactions in the middle temporal visual area of the owl monkey. *J Neurophysiol*, 84(5), 2658-2669.
- Brooks, B. A., & Fuchs, A. F. (1975). Influence of stimulus parameters on visual sensitivity during saccadic eye movement. *Vision Res*, 15(12), 1389-1398.

- Burr, D. C., & Morrone, M. C. (2010). Vision: keeping the world still when the eyes move. *Curr Biol*, 20(10), R442-444.
- Burr, D. C., Morrone, M. C., & Ross, J. (1994). Selective suppression of the magnocellular visual pathway during saccadic eye movements. *Nature*, 371(6497), 511-513.
- Campbell, F. W., & Wurtz, R. H. (1978). Saccadic omission: why we do not see a grey-out during a saccadic eye movement. *Vision Res*, 18(10), 1297-1303.
- Coppola, D., & Purves, D. (1996). The extraordinarily rapid disappearance of entopic images. *Proc Natl Acad Sci U S A*, 93(15), 8001-8004.
- Dayan, P., Abbott, L.F. (2001). Neural Encoding I: Firing Rates and Spike Statistics *Theoretical Neural: Computational and Mathematical Modeling of Neural Systems* (pp. 19-22): MIT Press.
- Ditchburn, R. W., & Ginsborg, B. L. (1952). Vision with a stabilized retinal image. *Nature*, 170(4314), 36-37.
- Ditchburn, R. W., & Ginsborg, B. L. (1953). Involuntary eye movements during fixation. *J Physiol*, 119(1), 1-17.
- Eizenman, M., Hallett, P. E., & Frecker, R. C. (1985). Power spectra for ocular drift and tremor. *Vision Res*, 25(11), 1635-1640.
- Gerrits, H. J., & Vendrik, A. J. (1974). The influence of stimulus movements on perception in parafoveal stabilized vision. *Vision Res*, 14(2), 175-180.

- Hafed, Z. M., Goffart, L., & Krauzlis, R. J. (2009). A neural mechanism for microsaccade generation in the primate superior colliculus. *Science*, *323*(5916), 940-943.
- Hurlimann, F., Kiper, D. C., & Carandini, M. (2002). Testing the Bayesian model of perceived speed. *Vision Res*, *42*(19), 2253-2257.
- Kagan, I., Gur, M., & Snodderly, D. M. (2008). Saccades and drifts differentially modulate neuronal activity in V1: effects of retinal image motion, position, and extraretinal influences. *J Vis*, *8*(14), 19 11-25.
- Kerzel, D., Aivar, M. P., Ziegler, N. E., & Brenner, E. (2006). Mislocalization of flashes during smooth pursuit hardly depends on the lighting conditions. *Vision Res*, *46*(6-7), 1145-1154.
- Lagae, L., Raiguel, S., & Orban, G. A. (1993). Speed and direction selectivity of macaque middle temporal neurons. *J Neurophysiol*, *69*(1), 19-39.
- Leopold, D. A., & Logothetis, N. K. (1998). Microsaccades differentially modulate neural activity in the striate and extrastriate visual cortex. *Exp Brain Res*, *123*(3), 341-345.
- Lisberger, S. G., & Movshon, J. A. (1999). Visual motion analysis for pursuit eye movements in area MT of macaque monkeys. *J Neurosci*, *19*(6), 2224-2246.
- Lisberger, S. G., & Westbrook, L. E. (1985). Properties of visual inputs that initiate horizontal smooth pursuit eye movements in monkeys. *J Neurosci*, *5*(6), 1662-1673.

- Martinez-Conde, S., Macknik, S. L., & Hubel, D. H. (2000). Microsaccadic eye movements and firing of single cells in the striate cortex of macaque monkeys. *Nat Neurosci*, 3(3), 251-258.
- Martinez-Conde, S., Macknik, S. L., & Hubel, D. H. (2002). The function of bursts of spikes during visual fixation in the awake primate lateral geniculate nucleus and primary visual cortex. *Proc Natl Acad Sci U S A*, 99(21), 13920-13925.
- Martinez-Conde, S., Macknik, S. L., & Hubel, D. H. (2004). The role of fixational eye movements in visual perception. *Nat Rev Neurosci*, 5(3), 229-240.
- Matin, E., Clymer, A. B., & Matin, L. (1972). Metacontrast and saccadic suppression. *Science*, 178(57), 179-182.
- Maunsell, J. H., & Van Essen, D. C. (1983). Functional properties of neurons in middle temporal visual area of the macaque monkey. I. Selectivity for stimulus direction, speed, and orientation. *J Neurophysiol*, 49(5), 1127-1147.
- Murakami, I., & Cavanagh, P. (1998). A jitter after-effect reveals motion-based stabilization of vision. *Nature*, 395(6704), 798-801.
- Newsome, W. T., & Pare, E. B. (1988). A selective impairment of motion perception following lesions of the middle temporal visual area (MT). *J Neurosci*, 8(6), 2201-2211.
- Newsome, W. T., Wurtz, R. H., Dursteler, M. R., & Mikami, A. (1985). Deficits in visual motion processing following ibotenic acid lesions of the middle temporal visual area of the macaque monkey. *J Neurosci*, 5(3), 825-840.

- Olveczky, B. P., Baccus, S. A., & Meister, M. (2003). Segregation of object and background motion in the retina. *Nature*, *423*(6938), 401-408.
- Orban, G. A., Kennedy, H., & Bullier, J. (1986). Velocity sensitivity and direction selectivity of neurons in areas V1 and V2 of the monkey: influence of eccentricity. *J Neurophysiol*, *56*(2), 462-480.
- Orban, G. A., Kennedy, H., & Maes, H. (1981). Response to movement of neurons in areas 17 and 18 of the cat: velocity sensitivity. *J Neurophysiol*, *45*(6), 1043-1058.
- Pitkow, X., Sompolinsky, H., & Meister, M. (2007). A neural computation for visual acuity in the presence of eye movements. *PLoS Biol*, *5*(12), e331.
- Raiguel, S., Van Hulle, M. M., Xiao, D. K., Marcar, V. L., & Orban, G. A. (1995). Shape and spatial distribution of receptive fields and antagonistic motion surrounds in the middle temporal area (V5) of the macaque. *Eur J Neurosci*, *7*(10), 2064-2082.
- Ramachandran, R., & Lisberger, S. G. (2005). Normal performance and expression of learning in the vestibulo-ocular reflex (VOR) at high frequencies. *J Neurophysiol*, *93*(4), 2028-2038.
- Ratliff, F., & Riggs, L. A. (1950). Involuntary motions of the eye during monocular fixation. *J Exp Psychol*, *40*(6), 687-701.
- Reppas, J. B., Usrey, W. M., & Reid, R. C. (2002). Saccadic eye movements modulate visual responses in the lateral geniculate nucleus. *Neuron*, *35*(5), 961-974.

- Riggs, L. A., Armington, J. C., & Ratliff, F. (1954). Motions of the retinal image during fixation. *J Opt Soc Am*, 44(4), 315-321.
- Riggs, L. A., & Ratliff, F. (1951). Visual acuity and the normal tremor of the eyes. *Science*, 114(2949), 17-18.
- Riggs, L. A., Ratliff, F., Cornsweet, J. C., & Cornsweet, T. N. (1953). The disappearance of steadily fixated visual test objects. *J Opt Soc Am*, 43(6), 495-501.
- Rodman, H. R., & Albright, T. D. (1987). Coding of visual stimulus velocity in area MT of the macaque. *Vision Res*, 27(12), 2035-2048.
- Rucci, M., & Desbordes, G. (2003). Contributions of fixational eye movements to the discrimination of briefly presented stimuli. *J Vis*, 3(11), 852-864.
- Rucci, M., Iovin, R., Poletti, M., & Santini, F. (2007). Miniature eye movements enhance fine spatial detail. *Nature*, 447(7146), 851-854.
- Sasaki, Y., Murakami, I., Cavanagh, P., & Tootell, R. H. (2002). Human brain activity during illusory visual jitter as revealed by functional magnetic resonance imaging. *Neuron*, 35(6), 1147-1156.
- Schutz, A. C., Braun, D. I., Kerzel, D., & Gegenfurtner, K. R. (2008). Improved visual sensitivity during smooth pursuit eye movements. *Nat Neurosci*, 11(10), 1211-1216.
- Skavenski, A. A., Robinson, D. A., Steinman, R. M., & Timberlake, G. T. (1975). Miniature eye movements of fixation in rhesus monkey. *Vision Res*, 15(11), 1269-1273.

Snodderly, D. M., Kagan, I., & Gur, M. (2001). Selective activation of visual cortex neurons by fixational eye movements: implications for neural coding. *Vis Neurosci*, *18*(2), 259-277.

Snowden, R. J., Treue, S., & Andersen, R. A. (1992). The response of neurons in areas V1 and MT of the alert rhesus monkey to moving random dot patterns. *Exp Brain Res*, *88*(2), 389-400.

Spauschus, A., Marsden, J., Halliday, D. M., Rosenberg, J. R., & Brown, P. (1999). The origin of ocular microtremor in man. *Exp Brain Res*, *126*(4), 556-562.

Spring, M., Kerzel, D., Braun, D. I., Hawken, M. J., & Gegenfurtner, K. R. (2005). Effects of contrast on smooth pursuit eye movements. *J Vis*, *5*(5), 455-465.

Steinman, R. M., Haddad, G. M., Skavenski, A. A., & Wyman, D. (1973). Miniature eye movement. *Science*, *181*(102), 810-819.

Stocker, A. A., & Simoncelli, E. P. (2006). Noise characteristics and prior expectations in human visual speed perception. *Nat Neurosci*, *9*(4), 578-585.

Stone, L. S., & Thompson, P. (1992). Human speed perception is contrast dependent. *Vision Res*, *32*(8), 1535-1549.

Tanaka, K., Hikosaka, K., Saito, H., Yukiie, M., Fukada, Y., & Iwai, E. (1986). Analysis of local and wide-field movements in the superior temporal visual areas of the macaque monkey. *J Neurosci*, *6*(1), 134-144.

Thiele, A., Henning, P., Kubischik, M., & Hoffmann, K. P. (2002). Neural mechanisms of saccadic suppression. *Science*, 295(5564), 2460-2462.

Thompson, P. (1982). Perceived rate of movement depends on contrast. *Vision Res*, 22(3), 377-380.

Turano, K. A., & Heidenreich, S. M. (1999). Eye movements affect the perceived speed of visual motion. *Vision Res*, 39(6), 1177-1187.

Tychsen, L., & Lisberger, S. G. (1986). Visual motion processing for the initiation of smooth-pursuit eye movements in humans. *J Neurophysiol*, 56(4), 953-968.

van Beers, R. J., Wolpert, D. M., & Haggard, P. (2001). Sensorimotor integration compensates for visual localization errors during smooth pursuit eye movements. *J Neurophysiol*, 85(5), 1914-1922.

Weiss, Y., Simoncelli, E. P., & Adelson, E. H. (2002). Motion illusions as optimal percepts. *Nat Neurosci*, 5(6), 598-604.

Zuber, B. L., & Stark, L. (1965). Microsaccades and the velocity-amplitude relationship for saccadic eye movements. *Science*, 150(702), 1459-1460.

Chapter 3: Noise correlations between responses of MT neurons and initiation of smooth pursuit eye movements

Abstract

The precision of a movement is necessarily limited by the precision of the motor command issued to the muscles that execute that movement. What limits the precision of the motor command? Because neural noise can propagate across synapses, the precision of the motor command might be inherited from upstream brain areas that play a critical role in providing signals to form an appropriate motor command. Here we asked whether sensory neurons contribute to noise in motor behavior by analyzing trial-by-trial fluctuations in single neurons in visual area MT during smooth pursuit eye movements. Fluctuations in sensory responses to repeated presentations of identical stimuli were correlated with deviations in eye speed at the initiation of pursuit. These correlations were strongest at the onset of both the neural and behavioral responses and depended on the direction of the stimulus relative to the preferred direction of the neurons. The observed correlation structure was inconsistent with common readout models of speed such as standard vector averaging or maximum likelihood estimation. Instead, we demonstrate that modifications of standard vector averaging involving motion opponent signals can account for the patterns of correlations. We also discuss a possible role of correlations in the timing of the neural and behavioral responses in shaping the structure of neuron-behavioral correlations. Further, we show that the variance of many neurons is only moderately larger than the variance in eye speed during pursuit initiation, which together with the existence of neuron-behavior correlations suggests that limited noise is added downstream from MT as the motor command is formed. Our results indicate that sensory noise propagates through the smooth pursuit system and contributes to variability in the oculomotor response.

Introduction

Movements are variable, no matter how often we practice them. The source of motor variation remains a matter of debate and could involve a number of neural and non-neural processes. Indeed, each movement results from a complex chain of events that begins with the processing of sensory inputs and ends with the contraction of the muscles that generate the desired movement. Any step along this chain could contribute to the variability of the final movement.

In the simplest case, motor variation could arise due to limitations in the ability of muscles to execute a precise, desired motor command. However, while variation in the force of muscular contraction is likely to add to motor variation, it is scarcely the sole contributor. At least in part, muscle variability is a consequence of variability in the motor commands themselves, as represented in the firing of motor neurons (Faisal, Selen, & Wolpert, 2008; Harris & Wolpert, 1998; van Beers, Haggard, & Wolpert, 2004). In turn, variability in motor commands could be inherited from upstream areas involved in planning the movement (Churchland, Afshar, & Shenoy, 2006; Medina & Lisberger, 2007; Schoppik, Nagel, & Lisberger, 2008) or areas representing the sensory evidence that guides the formation of the motor plan (Osborne, Hohl, Bialek, & Lisberger, 2007; Osborne, Lisberger, & Bialek, 2005). Understanding where and how motor variability arises is likely to shed light on fundamental questions of the nature of the neural code underlying the formation of a motor command.

As we interact with our environment, sensory neurons inform the brain about the world around us. Motor pathways must interpret these signals to generate precise

behaviors. Because the responses of single neurons are variable, downstream areas must pool signals across many sensory neurons in order to obtain an accurate estimate of the sensory parameters necessary for guiding our movements. In addition, the frame of reference in which sensory neurons encode parameters is generally different than that used by motor neurons to control the muscles (Groh, 2001; Lisberger, 2010). Therefore neural pathways controlling behaviors that rely on our senses are required to transform the pooled responses of the sensory neurons into a meaningful signal for the motor neurons. Studying the transformation of variability along a sensory-motor pathway informs us about possible computations underlying the conversion of sensory signals into a command for motor behavior.

Similar questions have been addressed in the context of simple perceptual decisions, which are variable from trial to trial for repeated presentations of identical stimuli (Britten, Newsome, Shadlen, Celebrini, & Movshon, 1996; Britten, Shadlen, Newsome, & Movshon, 1992; Dodd, Krug, Cumming, & Parker, 2001; Leopold & Logothetis, 1996; Logothetis & Schall, 1989; Newsome, Britten, & Movshon, 1989; Nienborg & Cumming, 2009; Purushothaman & Bradley, 2005; Ress & Heeger, 2003; Uka & DeAngelis, 2004). It was shown that the strength of inter-neuronal correlations, the size of the relevant neural pool, and the rules employed to read out the responses of upstream areas all have an impact on the propagation of neural noise (Shadlen, Britten, Newsome, & Movshon, 1996; Zohary, Celebrini, Britten, & Newsome, 1994). These factors may apply to motor systems as well. However, in contrast to discrete perceptual decisions, movements are continuous in nature and often operate on much faster time scales than have been studied in perceptual tasks.

Here we study the sensory contributions to motor variability in the smooth pursuit system. Smooth pursuit eye movements allow us to track an object with our eyes by keeping its image centered on the fovea, the high-acuity region of the retina. The pursuit system provides an excellent model for studying sensory-motor integration, the process by which the brain uses sensory information about the environment to guide motor responses. For smooth pursuit, both the sensory stages as well as the various areas involved in producing the motor command are relatively well understood (Krauzlis, 2004; Lisberger, 2010; Lisberger, Morris, & Tychsen, 1987). In the first ~120 ms of the smooth pursuit response, the eyes are driven purely by feed-forward sensory signals (Lisberger & Westbrook, 1985). These signals are provided by visual area MT, thus an ideal candidate for testing whether sensory neurons contribute to variability in the motor output.

We recorded responses from single neurons in area MT during smooth pursuit eye movements and asked whether trial-by-trial variability in MT responses predicts corresponding variability in pursuit eye velocity. Fluctuations in MT responses were correlated with fluctuations in the speed of pursuit eye movements and were strongest at the onset of both the neural and the behavioral responses. This result suggests that sensory noise can propagate through the brain to contribute to motor variability in the oculomotor system. Moreover, neuron-behavior correlations depended on the characteristics of the stimulus motion relative to the tuning properties of the MT neurons. Correlations were consistently positive when the stimulus moved in the preferred direction of the neurons and mostly negative when the stimulus moved in the opposite direction. Using a simulated population of MT neurons, we derived the predicted neuron-

behavior correlation structure for various models that have been suggested in the past for reading out speed from MT. Common models such as standard vector averaging or maximum likelihood were unable to explain the observed correlation structure in our data. Instead a modified vector averaging computation comparing opponent motion signals was necessary to reproduce the measured pattern of MT-pursuit correlations. Further, the variance in eye speed was approximately just ten times larger than the variance of single neuron responses in MT. This poor noise reduction along with the existence of MT-pursuit correlations suggests that limited noise is added downstream from MT during pursuit initiation.

Materials and Methods

Subjects

Eye movement traces and neural recordings were obtained from two adult male rhesus monkeys (*Macaca mulatta*, 7 and 13 kg). After basic training, monkeys were implanted with stainless steel or titanium head holders for head fixation and scleral search coils for recording eye movements. Technical details have been described previously (Ramachandran & Lisberger, 2005). Titanium or cilux recording chambers (Crist instruments, Hagerstown, MD) were mounted over a 20 mm circular opening in the skull to allow access to MT for neural recordings. For each experimental session, monkeys sat in a primate chair and received fluid rewards for accurately fixating or tracking visual targets presented on a screen in front of them. All surgical and experimental procedures were approved in advance by the Institutional *Animal Care and Use Committee* of the University of California, San Francisco and were in strict compliance with the *NIH Guide for the Care and Use of Laboratory Animals*.

Visual stimuli

All experiments were conducted in a nearly dark room. Visual stimuli were presented on an analog oscilloscope (Hewlett Packard 1304A) with a refresh rate of 250 Hz. The oscilloscope was driven by 16-bit digital-to-analog converters on a digital signal processing board in a PC. The display was positioned 20.5 cm from the monkey and subtended a 67° horizontal by 54° vertical visual angle.

For mapping receptive fields of neurons in MT, a small bright spot was presented at the center of the screen. The monkey was required to maintain gaze within one degree

of this fixation point. After manually locating the receptive field, the direction and speed tuning of each neuron was measured by placing a patch of moving random dots in the receptive field of the neuron. Random dot patches approximately matched the size of the receptive fields of the neurons and were $5 \times 5^\circ$ or $8 \times 8^\circ$ large apertures containing dots placed at random locations with a density of 2 dots/deg². During each stimulus presentation, dots moved coherently in a given direction at a specified speed for 300 ms and vanished for 200 ms before reappearing at the same location, but moving either at a different speed (speed tuning) or in a different direction (direction tuning). Five different directions or speeds were presented in random order within a single behavioral trial before the monkey received a reward for maintaining proper fixation.

Pursuit trials began with a small square of $0.3 \times 0.3^\circ$ appearing in the center of the screen serving as the fixation target (Figure 3.1). The square shape of the fixation target cued the monkey to expect a pursuit trial. Following a random delay of 500-900 ms, a $5 \times 5^\circ$ or $8 \times 8^\circ$ static random dot patch appeared in the receptive field of the neuron. After another random delay of 300-900 ms, the dots began moving coherently. Both delays were drawn from uniform distributions. The delay between dot onset and dot motion allowed us to isolate the MT response to motion from the transient caused in many neurons by the onset of a visual stimulus. The onset of dot motion coincided with the disappearance of the fixation target, cueing the monkey to pursue the patch.

Crucially, the first 100 ms after fixation target disappearance consisted of 'local motion' only, i.e. the dots moved within a static aperture. This segment of local motion, which is barely discriminable from *en bloc* "global" motion of dots and aperture, evokes pursuit responses equal to those elicited by global motion as long as the local and global

motion vectors are identical (Osborne et al., 2007). Adding this segment allowed us to keep the stimulus in the receptive field of the neuron during the delay between motion and pursuit onset. After 100 ms of local motion, the aperture started moving at the same speed and in the same direction as the dots, typically for 250-500 ms depending on the speed of the target. Monkeys received fluid rewards for keeping their eyes within 3-5° of target position throughout the pursuit portion of the trial. The exact fixation requirement depended on the speed and the size of the pursuit target as well as the starting location of the patch relative to the fixation target.

These parameters of target motion had to be adjusted depending on the receptive field location and properties of the neuron under study. We ensured that the chosen parameters allowed saccade-free pursuit initiation, and we were not concerned about the exact location of the eye within the patch during pursuit. Typically, 4-6 stimulus conditions, each with different directions or speeds of motion, were randomly interleaved in a block of trials. Each stimulus condition was balanced by another condition in which the target moved at equal speed and opposite direction to prevent anticipatory pursuit responses. Monkeys usually completed 2000-3600 pursuit trials in each daily experiment.

MT recording

We recorded responses of 104 neurons in visual area MT of two monkeys (52 neurons each in monkeys Y and J). We used a Thomas microdrive (Thomas Mini-Matrix 05, Thomas Recording, Giessen, Germany) to lower quartz-shielded tungsten electrodes vertically into MT. Electrode impedances ranged from 1 to 4 M Ω . MT was identified based on stereotaxic coordinates, directional and speed response properties of neurons, receptive field sizes, retinotopic organization, and surrounding cortical areas (Desimone

& Ungerleider, 1986; Maunsell & Van Essen, 1983). We typically recorded from neurons with receptive field centers within the central 5° of the visual field.

Electrical signals were amplified and digitized for on-line spike sorting and spikes were initially assigned to single neurons by using a template-matching algorithm (Plexon MAP, Plexon Inc., Dallas, TX). After the experiment, we used a combination of visual inspection of waveforms, projection onto principal components, template-matching, and refractory period violations in Offline Sorter (Plexon Inc, Dallas, TX) to sort and assign spikes to well isolated single units. After sorting, waveforms were converted to timestamps with 1 ms precision for analysis. Firing rates were obtained by convolving spikes trains with a Gaussian window of 10 ms standard deviation.

To obtain the tuning properties of each cell, we fit speed and direction tuning curves with Gaussian functions (Lisberger & Movshon, 1999):

$$\text{Speed tuning curve: } R(s) = R_0 + a * \exp \left\{ - \left[\frac{\log\left(\frac{s}{ps}\right)}{\sigma_s + d * \log\left(\frac{s}{ps}\right)} \right]^2 \right\} \quad (1)$$

$$\text{Direction tuning curve: } R(\theta) = R_0 + A * \exp \left\{ - \frac{1}{2} \left[\frac{\theta - p\theta}{\sigma_\theta} \right]^2 \right\} \quad (2)$$

(s – speed, θ – direction, R_0 – baseline firing rate, a – amplitude of speed tuning curve, A – amplitude of direction tuning curve, ps – preferred speed, $p\theta$ – preferred direction, σ_s – width of speed tuning curve, σ_θ – width of direction tuning curve, and d – skew parameter of speed tuning curve). The angle $\theta - p\theta$ was restricted to be within $[-\pi, \pi]$ degrees.

Behavioral data

Eye position and velocity signals were sampled and stored at 1000 Hz. Velocity traces were smoothed with a zero-phase, 25 Hz, 2-pole digital Butterworth filter. Before analysis, each trial record was inspected and rejected if a saccade occurred within the time window chosen for analysis. Data sets contained at least 80 and typically 300 repetitions of each trial condition.

MT-pursuit correlations were calculated to characterize the relationship between the trial-by-trial variation in the firing rates of single neurons and the trial-by-trial variation eye speed during pursuit initiation. Experiments usually contained a small number of interleaved target motions, and we computed the MT-pursuit correlations for each target motion separately. Although we only included trials that did not contain saccades or microsaccades during fixation, we observed that small fluctuations in fixation eye velocity can contribute to neuron-behavior correlations. Therefore, we removed temporal autocorrelations in eye speed to report the fraction of MT-pursuit correlations that was not related to fixation eye movements. We removed correlations between fixation and pursuit eye speed only and left MT responses untouched because this method quantified most accurately the true MT-pursuit correlations in our data. The alternative approach of removing correlations between MT firing rates and fixation eye speed introduces errors that could affect the value of the MT-pursuit correlations because firing rates are not Gaussian distributed at motion onset. However, our results did not change qualitatively when we removed correlations with fixation eye velocity both from pursuit eye speed and neural responses.

To account for temporal auto-correlations in eye speed, we built linear predictions of eye speed during the initial pursuit response (80-120 ms after motion onset) based on eye speed during fixation (-40 to 40 ms relative to motion onset). These predictions were subtracted from the initial pursuit response to obtain a "decorrelated" or residual eye speed, which was then used to calculate MT-pursuit correlations. To construct the linear prediction, we chose the time interval during fixation that was maximally predictive of pursuit eye speed; however, our results were insensitive to the exact fixation time window chosen as long as it included the time interval around motion onset. For time intervals occurring later than 120 ms after pursuit onset the filter had little predictive power and removing predictions had no significant effect on the results.

The linear filter we constructed is the analytical solution to a multilinear regression between fixation and pursuit eye speed and is optimal in the least squared sense. This method has been applied previously in other contexts (Warland, Reinagel, & Meister, 1997). One assumption of this method is that the independent variables, in our case eye velocity at different times during fixation, are uncorrelated with each other. To minimize the correlation between sequential time points in eye velocity, we downsampled our data by calculating the mean over 20 ms time bins. To confirm that this was sufficient, we calculated filters based on ridge regression and the predictions were virtually identical.

Predictions were obtained in the following way: \mathbf{V}_{fix} is the matrix describing eye velocity during fixation with trials in rows and time points in columns, h_j^i is the horizontal, and v_j^i the vertical eye speed during trial i at time point j . \mathbf{V}_{purs} describes

horizontal and vertical pursuit eye speeds (h_p^i and v_p^i) during 80-120 ms after motion onset. Because we considered only residuals, there is no constant term in \mathbf{V}_{fix} .

$$\mathbf{V}_{\text{fix}} = \begin{bmatrix} h_1^1 & h_2^1 & \cdots & h_n^1 & v_1^1 & v_2^1 & \cdots & v_n^1 \\ h_1^2 & h_2^2 & \cdots & h_n^2 & v_1^2 & v_2^2 & \cdots & v_n^2 \\ \vdots & \vdots & \ddots & \vdots & \vdots & \vdots & \ddots & \vdots \\ h_1^m & h_2^m & \cdots & h_n^m & v_1^m & v_2^m & \cdots & v_n^m \end{bmatrix}, \mathbf{V}_{\text{purs}} = \begin{bmatrix} h_p^1 & v_p^1 \\ h_p^2 & v_p^2 \\ \vdots & \vdots \\ h_p^m & v_p^m \end{bmatrix} \quad (2.5)$$

Pursuit predictions were obtained by calculating the filter \mathbf{f} :

$$\mathbf{f} = (\mathbf{V}_{\text{fix}}^T \mathbf{V}_{\text{fix}})^{-1} \cdot (\mathbf{V}_{\text{fix}}^T \mathbf{V}_{\text{purs}}) \quad (3)$$

$$\mathbf{V}_{\text{purs}}^{\text{pred}} = \mathbf{V}_{\text{fix}} \cdot \mathbf{f} \quad (4)$$

$$\mathbf{V}_{\text{purs}}^{\text{decorr}} = \mathbf{V}_{\text{purs}} - \mathbf{V}_{\text{purs}}^{\text{pred}} \quad (5)$$

Finally, for calculating correlations with firing rates, we converted the horizontal and vertical components of $\mathbf{V}_{\text{purs}}^{\text{decorr}}$ into the absolute value of decorrelated eye speed.

Simulations

Model population. We simulated a population of correlated, noisy MT neurons with preferred speeds that uniformly tiled the log space between 0.5 and 512 deg/sec and preferred directions evenly distributed between -180 and 180 degrees. The simulations underlying all plots in this paper were based on a pool of $N_{\text{ps}} \times N_{\text{pd}}$ neurons, with $N_{\text{ps}} = N_{\text{pd}} = 60$, where N_{ps} describes the number of different preferred speeds and N_{pd} the number of different preferred directions. The mean response R_{mean} of each neuron was

determined by the sum of the baseline activity R_0 and the product of the direction and speed tuning curve.

$$R_{mean}(\theta, s) = R_0 + g^* \exp \left\{ -\frac{1}{2} \left[\left(\frac{\log\left(\frac{s}{ps}\right)}{\sigma_s} \right)^2 + \left(\frac{\theta - p\theta}{\sigma_\theta} \right)^2 \right] \right\} \quad (6)$$

The parameters s and θ describe the stimulus speed and direction, ps and $p\theta$ the preferred speed and preferred direction of the neuron. The amplitude g as well as the bandwidth σ_s of the speed tuning and σ_θ of the direction tuning was kept constant across the neural population. ($R_0 = 1$, $\sigma_s = 1.5$, $\sigma_\theta = 40$, $g = 10$). The angle $\theta - p\theta$ was restricted to be within the interval $[-\pi, \pi]$.

On every trial we added to each neuron's mean response correlated noise drawn from a normal distribution with the variance scaled to the mean response. The expected correlation structure r_{ij} between neurons i and j was:

$$r_{i,j} = r_{max} \exp \left\{ -\left[\left(\frac{p\theta_i - p\theta_j}{\tau_\theta} \right)^2 + \left(\frac{\log_2\left(\frac{ps_i}{ps_j}\right)}{\tau_s} \right)^2 \right] \right\} \quad (7)$$

The parameters r_{max} (peak correlation), τ_s and τ_θ (width of the correlation structure as a function of speed and direction) were chosen so that the neuron-neuron correlations in the model MT population matched the experimental data measured previously (Huang & Lisberger, 2009) ($r_{max} = 0.78$, $\tau_s = 2$, $\tau_\theta = 40$). We followed the methods of Shadlen et al.

(1996) to produce correlated deviates on each trial that on average produced the neuron-neuron correlation described by the equation above.

We used the following decoding models to test the neuron-behavior correlation structure predicted from the model MT population responses:

Standard vector averaging (Groh, Born, & Newsome, 1997; Lisberger & Ferrera, 1997; Priebe & Lisberger, 2004; Salinas & Abbott, 1994):

$$\hat{s} = \frac{\sum_i R_i \log_2(p s_i)}{\sum_i R_i}, s = 2^{\hat{s}} \quad (8)$$

s is the readout of speed, and R_i the response of the i^{th} neuron.

Vector averaging, opponent (Churchland & Lisberger, 2001; Huang & Lisberger, 2009; Yang & Lisberger, 2009): Opponent vector averaging was implemented by weighting responses in the numerator by the sine and cosine of preferred direction. The use of the trigonometric functions naturally creates opponency between neurons that prefer opposite directions. Horizontal and vertical eye speeds s_h and s_v were decoded separately before combining these values to the total speed s .

$$s_h = \frac{\sum_i \cos(p\theta_i) R_i \log_2(p s_i)}{\sqrt{R_h^2 + R_v^2}} \quad (9)$$

$$s_v = \frac{\sum_i \sin(p\theta_i) R_i \log_2(p s_i)}{\sqrt{R_h^2 + R_v^2}} \quad (10)$$

$$s = 2\sqrt{s_h^2 + s_v^2} \quad (11)$$

where $R_h = \sum_i \cos(p\theta_i)R_i$ and $R_v = \sum_i \sin(p\theta_i)R_i$

Vector averaging, numerator opponent (Churchland & Lisberger, 2001): This readout differs from opponent vector averaging by its denominator.

$$s_h = \frac{\sum_i \cos(p\theta_i)R_i \log_2(ps_i)}{k \sum_i R_i} \quad (12)$$

$$s_v = \frac{\sum_i \sin(p\theta_i)R_i \log_2(ps_i)}{k \sum_i R_i} \quad (13)$$

$$s = 2\sqrt{s_h^2 + s_v^2} \quad (14)$$

The constant k ensures that the readout scales with stimulus speed.

Maximum likelihood (Deneve, Latham, & Pouget, 1999): Under the assumption of a uniform prior, we computed the likelihood function for speed readout as:

$$LH(s, \theta) \propto \frac{\exp\left[-\frac{1}{2}(\mathbf{a} - \mathbf{R}_{\text{mean}}(s, \theta))^T \mathbf{C}^{-1}(\mathbf{a} - \mathbf{R}_{\text{mean}}(s, \theta))\right]}{\sqrt{(2\pi)^N \det \mathbf{C}}} \quad (15)$$

where \mathbf{a} is the vector of neural responses on a given trial, $\mathbf{R}_{\text{mean}}(s, \theta)$ is a vector describing the mean response of the population determined by equation (6) above, and \mathbf{C}

is the matrix describing the structure of the covariance among neurons in our model population.

Correlated latencies: As a control, we also used our experimental data to evaluate the MT-pursuit correlations that would be expected if the temporal onset of the neural response were correlated with the temporal onset of the pursuit response. Within each stimulus condition, we first shuffled the eye velocity and firing rate across trials to remove MT-pursuit correlations. Then, we introduced a coherent latency shift in both firing rate and eye speed for each trial by drawing values from a Gaussian distribution of zero mean and 5 ms standard deviation. Finally, we computed the MT-pursuit correlations using our original analysis procedure. Using shuffled data to test the latency hypothesis had two advantages: shuffling eliminated any correlations in our data while naturally leaving variance in timing onset in both the neural and speed traces. Thus the realigned data contained a correlated (shared) and an uncorrelated (noisy) component between firing rate and eye speed, similar to the timing that presumably exists in the real data. Because it is difficult to determine the onset of pursuit and neural responses with 1 ms precision from single trial traces, we did not attempt the alternative of performing the MT-pursuit correlation analysis after aligning data to the onset of both firing rate and pursuit for each trial.

Results

We used a modified step-ramp pursuit task (Osborne et al., 2007; Rashbass, 1961) to study correlations between firing rates of single neurons in visual area MT and speed of smooth pursuit eye movements. A patch of random dots, which elicits robust responses in MT neurons, served as our pursuit target. Each trial consisted of three distinct epochs (Figure 3.1). First, the dots appeared in the MT receptive field and remained stationary for a variable amount of time (left). Next, the dots started moving locally within the receptive field while the aperture containing the dots remained stationary (local motion, middle). Finally, the aperture itself began moving at the same speed as the dots (right). The short epoch of local motion is effective at driving an initial pursuit response (Osborne et al., 2007; Priebe, Churchland, & Lisberger, 2001) and ensured that the patch was centered on the receptive field of the neuron until the eyes started moving. On each trial, both the speed and direction of motion of the dots were chosen randomly from a set of target motions falling either on the peaks or the flanks of the direction- and speed-tuning curves of the neuron under study.

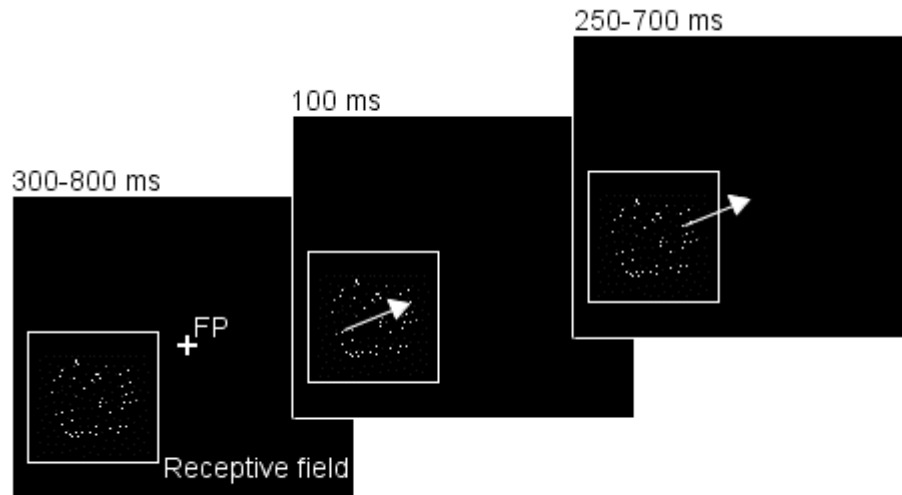


Figure 3.1.

The pursuit task. Left: Once the monkey acquired fixation on a point (FP) at the center of the screen, a patch of random dots appeared in the receptive field of the neuron. This patch remained stationary for a randomized amount of time between 300-800ms (fixation segment). Middle: The fixation point disappeared, cueing the monkey to initiate pursuit. At the same time the dots started moving coherently for 100ms within the static aperture of the patch (local motion segment). Right: The patch moved at the same speed and in the same direction as the dots for a fixed time between 250-700ms, depending on the speed used in a particular experiment (global motion segment). The speed and direction of motion of the dots were the same during the local and global motion segment.

Even though our task provided compelling visual motion and the monkeys performed the behavioral task diligently, both eye movements and neural responses were somewhat variable from trial-to-trial for repeated presentations of identical stimuli and under identical instructions. Figure 3.2 shows simultaneous recordings of eye speed and spikes of a single MT neuron for five repetitions of the same stimulus.

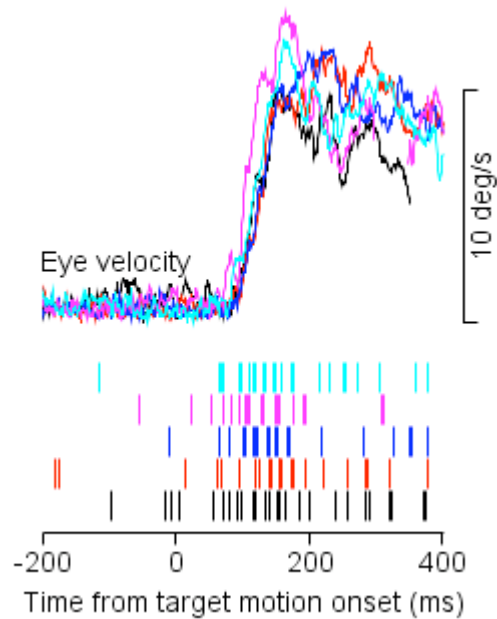


Figure 3.2.

Simultaneous recordings of smooth pursuit eye movements and neural responses. Example eye velocity traces are plotted as a function of time with trials aligned to stimulus motion onset at 0ms. Below the eye traces we plotted spikes for the same trials as above with matching colors indicating data collected on the same trials.

MT-pursuit correlations

Firing rates in MT were, in fact, correlated with eye speed on a trial-by-trial basis, and the correlations persisted after filtering to remove the effects of oscillations in eye speed during fixation (Figure 3.3). We computed correlations between firing rates (vertical axis) and eye speed (horizontal axis) averaged over short time-bins (20 ms) covering the time period around the onset of target motion. We first calculated correlations across trials collected under identical stimulus conditions, and then averaged the MT-pursuit correlations across conditions. For both monkeys, we observed strong positive correlations between the onset of the neural response to motion (20-60 ms after motion onset) and the beginning of the pursuit response (80-120 ms after motion onset). Because the neural responses precede the eye movement at these time points, the observed correlations are consistent with a causal influence of MT responses on eye speed. As we will discuss below, we observed these positive correlations only for stimuli moving at or around the preferred direction of the MT neuron.

For the same stimuli, we observed negative correlations during pursuit initiation when the neural response lagged the eye movements (Figure 3.3). These correlations are likely the result of a combination of effects due to the motion of the eyes during pursuit initiation. The faster the eyes catch up to the target, the slower the retinal image speed becomes and the sooner the stimulus moves outside of the MT receptive field. Both of these factors decrease MT responses, resulting in a negative correlation between eye speeds and firing rates. The timing of these negative correlations is inconsistent with a

causal role of MT responses on eye movements and will therefore not be discussed further.

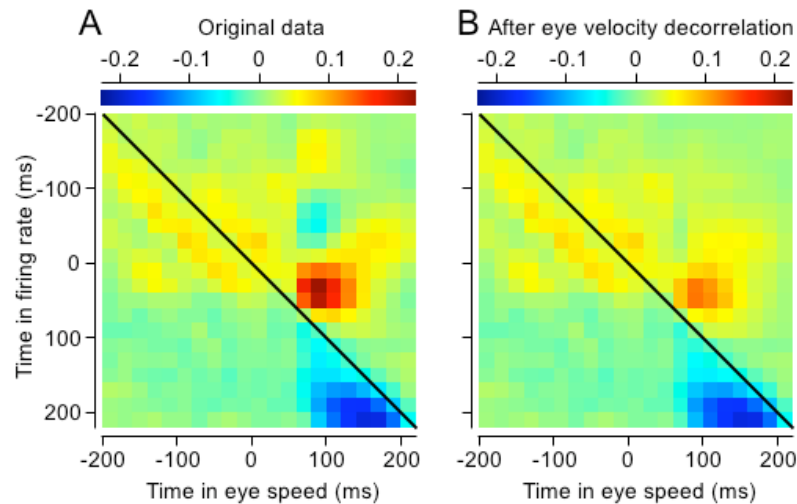


Figure 3.3.

Neuron-behavior correlations. Average correlation matrix between firing rate and eye speed for monkey J for targets moving within 90 degrees of preferred direction of neurons. The correlation matrix is the correlation coefficient between firing rate and eye speed between all time points in both the neural and behavioral response. Time in firing rate is shown on the vertical axis and time in eye speed runs along the horizontal axis. The values of the correlation coefficients are indicated in color. Points above the diagonal correspond to firing rates that precede eye movements. Left panel: Correlation matrix calculated on original data. Right panel: Correlation matrix after correlations between fixation and pursuit eye speed have been removed.

Removal of eye velocity temporal correlations

We have conducted some control analyses because the interpretation of the observed positive correlations is complicated by the presence of fixational eye movements that affect MT responses to motion onset as well as eye speed at the initiation of pursuit (Figure 3.4). Even during what appears to be steady fixation, the eyes are not stable, but rather oscillate at a frequency of about 4-5 Hz (Chapter 2). The eye movements of fixation introduce some variation in the eye velocity at the time of pursuit initiation that is correlated with variation in eye velocity during fixation. To illustrate the correlation (Figure 3.4A), we binned all individual trials in 13 groups according to the eye velocity at the time the visual stimulus started to move. We computed the residual eye velocity for each trial, defined as the actual minus the mean for its particular stimulus. We then averaged residual eye velocity along the preferred direction of the neuron under study and firing rate within each of the 13 groups of trials.

In Figure 3.4A, the ordering of eye velocity at the onset of stimulus motion agrees well with the order of the same eye velocity traces in the interval from 80 to 120 ms after the onset of stimulus motion, which is the interval that revealed strong MT-pursuit correlations. In addition, the variation in eye velocity across the 13 groups of trials during fixation is related to the responses of MT neurons to the onset of target motion in the same groups of trials. In the interval from 40-80 ms after stimulus motion onset (Figure 3.4C), MT responses are shifted toward later times as the eye velocity during fixation varies from decreasingly positive to zero to increasingly negative. Firing rate in the 13 groups follows the same order as eye velocity during fixation. Presented as residuals

relative to the mean firing rate across all trials (Figure 3.4D), the latency shifts amount to systematic changes in the magnitude of MT firing in the interval from 20 to 60 ms after the onset of stimulus motion.

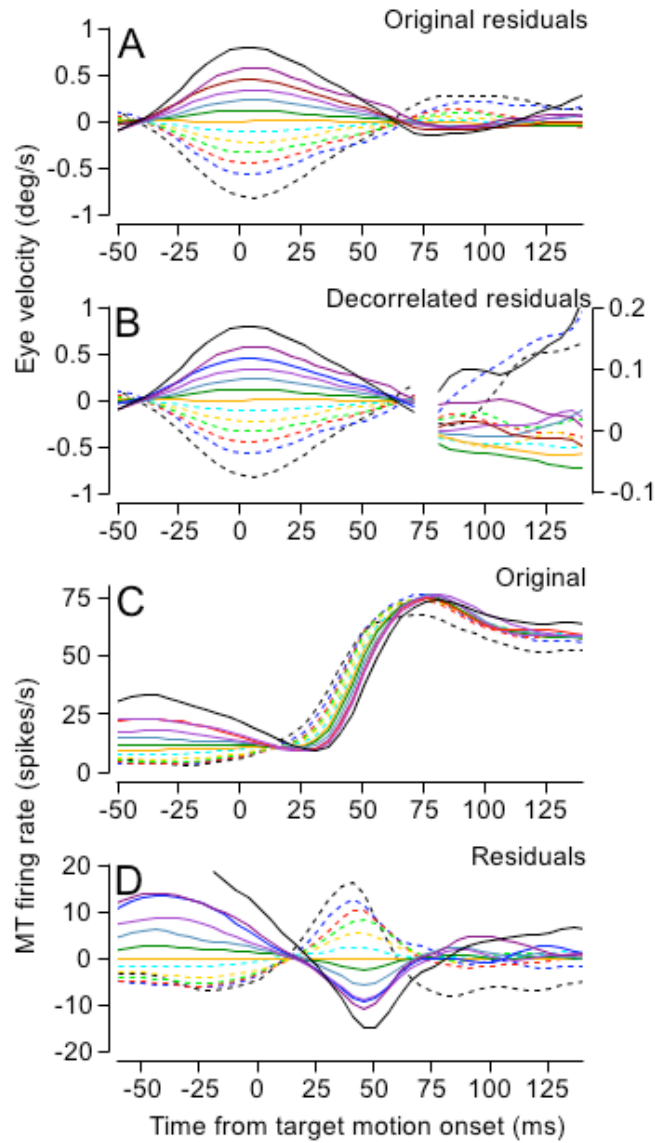


Figure 3.4.

Removing correlations due to small fluctuations in eye velocity during fixation. Eye velocity was projected onto the preferred direction of neurons in order to visualize the effect of fixation eye movements on firing rates and pursuit eye speed. Top row: Residual eye velocity - trials were grouped and averaged based on fluctuations in eye speed at the onset of motion in the stimulus (0 ms). The pursuit response begins around 80ms, but is not evident in the residual eye velocity traces because for each stimulus condition the average eye velocity was subtracted from every trial. Second row: Residual pursuit eye velocity - autocorrelations between fixation and pursuit eye speed were removed from pursuit eye velocity. Third row: Firing rates as a function of time for the same groups of trials as the first two rows. Bottom row: Firing rates grouped as above with mean firing rate subtracted.

We showed in Figure 3.3 that the eye movements of fixation contributed little to the MT pursuit correlations, and that a strong correlation persisted after we used a filtering procedure to remove the effect of eye velocity during fixation on eye velocity during the initiation of pursuit (compare Figures 3.3A and B). Figure 3.4B verifies that the decorrelation procedure worked. Here, the traces in the interval from -50 to 75 ms relative to the onset of target motion are the raw eye velocities measured in the 13 groups of trials during fixation. The higher magnification traces in the interval from 80 to 140 ms after the onset of target motion show that decorrelation abolished the ordering of the 13 groups of eye velocity during the initiation of pursuit, indicating that the correlation between the eye velocity of fixation and the eye velocity of the initiation of pursuit has been eliminated. Therefore, the existence of MT-pursuit correlations after decorrelation implies that the correlations are not caused by the small eye movements of fixation and

must be attributed to other mechanisms. For the remainder of the paper, we show only results obtained after decorrelation.

Structure of MT-pursuit correlations

MT neurons are tuned for the direction of stimulus motion and respond preferentially to visual motion along a particular axis, which is specific to each neuron (Albright, 1984; Lisberger & Movshon, 1999; Maunsell & Van Essen, 1983; Rodman & Albright, 1987; Snowden, Treue, & Andersen, 1992). In addition, neural responses in MT depend on the speed of visual motion (Lagae, Raiguel, & Orban, 1993; Lisberger & Movshon, 1999; Maunsell & Van Essen, 1983; Rodman & Albright, 1987). To define the structure of MT-pursuit correlations, we next analyze how the magnitude and sign of the MT-pursuit correlations depends on the relationship between the direction and speed of target motion, versus the preferred direction and speed of the neuron under study.

The magnitude and sign of the MT-pursuit correlations depended on the direction in which the stimulus moved relative to the preferred direction of a given neuron. We divided up the first 120 ms of the neural and pursuit responses into three consecutive 40 ms intervals and analyzed each interval separately (Fig. 3.5, top row). During the first 40 ms, the firing rates of a large percentage of neurons were positively correlated with eye speed when the target moved in the preferred direction of a neuron (mean neuron-behavior correlation coefficient $r_{NB} = 0.097$, 42.44% significant). Firing rates had a slight tendency to be negatively correlated when the target moved in the opposite direction (mean $r_{NB} -0.034$, 16.79% significant). During later time intervals, we observed fewer

significant correlations and the difference between motion in the preferred versus the opposite direction decreased.

In contrast to the findings for direction, the correlation coefficients depended little on the speed of the stimulus relative to the preferred speed of neurons. However, for all time intervals considered, the MT-pursuit correlation structure hardly depended on stimulus or preferred speed of the neurons (Figure 3.5, bottom row). As we will show below, models for decoding MT make specific predictions about the MT-pursuit correlation structure as a function of the tuning properties of MT neurons and we can compare these predictions with the correlations we measured.

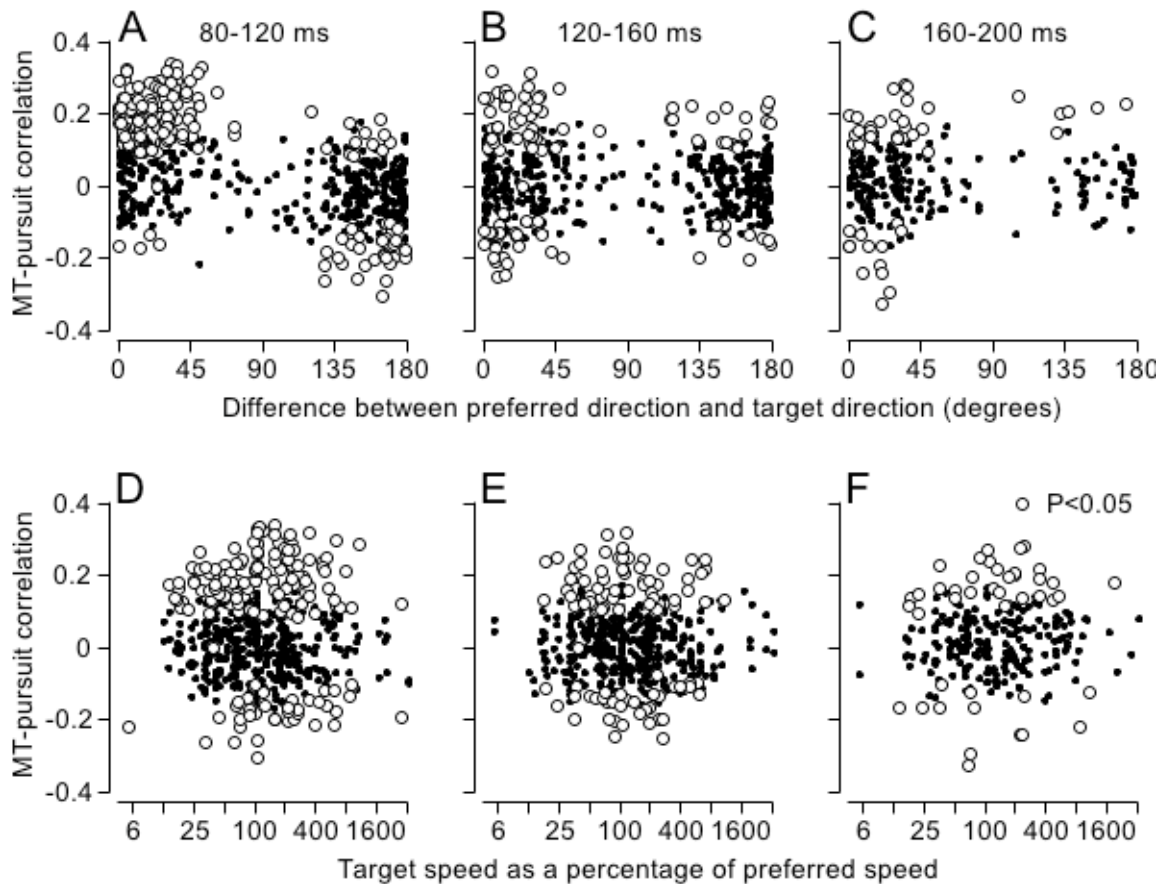


Figure 3.5.

MT-pursuit correlations as a function of the tuning properties of MT neurons. Correlation coefficients between firing rate and eye speed are plotted against the difference between preferred and target direction (top row) and against target speed as a percentage of preferred speed (bottom row). Each dot represents the correlation coefficient for one stimulus condition and neuron, and data is plotted for both monkeys. The lag between firing rate and eye speed was kept constant at 60 ms for all time intervals. The three columns describe correlations during subsequent time intervals with the time of pursuit eye speed labeled at the top.

Decoding model predictions

As described in the Methods, we created a population of model MT neurons that had the mean tuning curves, response variance, and noise correlations found in our recordings from area MT (Huang & Lisberger, 2009). We ran 1000 simulated trials for target motion at 16 deg/s, and created a separate instantiation of the model MT population for each trial. We next applied several different decoding computations described in the prior literature to each trial, and obtained estimates of target speed using the different decoding computations. Finally, we computed the trial-by-trial correlation between the responses of the model MT neurons and the estimates of target speed for each model neuron and each decoding computation.

To represent the structure of the MT-pursuit correlations in our data and compare them with the predictions of the different decoding computations, we developed the graphs shown in figure 3.6. Neurons were placed in bins according to their preferred speed and preferred direction, relative to target speed and direction. In figure 3.6A, the colors of each pixel indicate the mean MT-pursuit correlation in our data for neurons with the preferred speed and direction signified by the location of the pixel along the y-axis and x-axis. Figure 3.6A contains a non-white pixel only for the bins where we recorded neurons. In the other panels, which show the MT-pursuit correlations predicted by different decoding computations, we have colored only the pixels for which we had data in figure 3.6A, to allow a fair visual comparison. A glance at figure 3.6 reveals that the procedures used to obtain figure 3.6E and F did a reasonable job of reproducing the MT-pursuit correlations in our data, while the procedures used to obtain figures 3.6B, C, and D failed qualitatively. We elaborate below.

Standard vector averaging (Groh et al., 1997; Lisberger & Ferrera, 1997; Priebe & Lisberger, 2004; Salinas & Abbott, 1994) finds the center of mass of the responses of all MT neurons along the axis of preferred speed. The predicted MT-pursuit correlations for vector averaging (Figure 3.6B) were positive for neurons with preferred speeds higher than target speed and negative for model neurons with preferred speeds lower than target speed. In contrast to the predictions of standard vector averaging, the MT-pursuit correlations in our data did not change signs depending on whether the preferred speed of the neuron was above or below target speed. Given that our implementation of standard vector averaging ignores the direction tuning of the neurons, comparison with the data along the axis of preferred direction would not be meaningful.

We can understand intuitively the predictions of decoding with standard vector averaging. Vector averaging estimates speed based on the center of mass of the active neural population. On trials where neurons with low preferred speeds have higher firing rates than average, the center of mass is pulled towards lower preferred speeds resulting in smaller speed estimates and negative MT-pursuit correlations. On trials where neurons with high preferred speeds have higher firing rates than their average, the center of mass of the population is pulled towards higher preferred speeds resulting in higher speed estimates and positive MT-pursuit correlations. The MT-pursuit correlation crosses zero when preferred speed is the same as target speed because an increase or decrease in the firing rate of these neurons does not move the center of mass of the population response. Due to the presence of baseline activity in our simulated population, all neurons were active and therefore contributed to the speed estimate even if their preferred directions were opposite to the target direction.

Opponent vector averaging (Churchland & Lisberger, 2001; Huang & Lisberger, 2009; Yang & Lisberger, 2009) predicted the same MT pursuit correlations as did standard vector averaging for model neurons with preferred directions within 90 degrees of target direction (Figure 3.6C). The MT-pursuit correlations in our data (Figure 3.6A) did not resemble the predictions of opponent vector averaging. However, the reversal of MT-pursuit correlations for neurons with preferred directions far from versus near the direction of target motion suggests that a decoding computation with directional opponency may be successful at predicting our data. For the opponent vector averaging decoder, the combination of direction opponency in the decoder and the non-zero baseline rates of our model MT population create a reversal of the sign of the predicted MT-pursuit correlations for model neurons with preferred directions that differed from target direction by more than 90 degrees

A maximum likelihood decoder (Deneve et al., 1999) predicted a similar neuron-behavior correlation structure as standard vector averaging (Figure 3.6D), at least for model neurons with preferred directions within 90 degrees of target direction. In this range of preferred directions, the predictions from maximum likelihood decoding disagreed with the data. Initially, we were surprised that a maximum likelihood decoder that was privy to the structure of the neuron-neuron correlations would predict any MT-pursuit correlations at all. We expected the decoder to effectively eliminate shared noise in the MT population. As a consequence, we had expected that fluctuations from individual units would not propagate to the output and MT-pursuit correlations would be abolished. Instead, MT-pursuit correlations still appear, although they are smaller than those resulting from a maximum likelihood decoder that ignores neuron-neuron

correlations (data not shown). Therefore a maximum likelihood decoder that knows about the neuron-neuron correlation structure can reduce the effect of shared noise, but cannot remove it entirely.

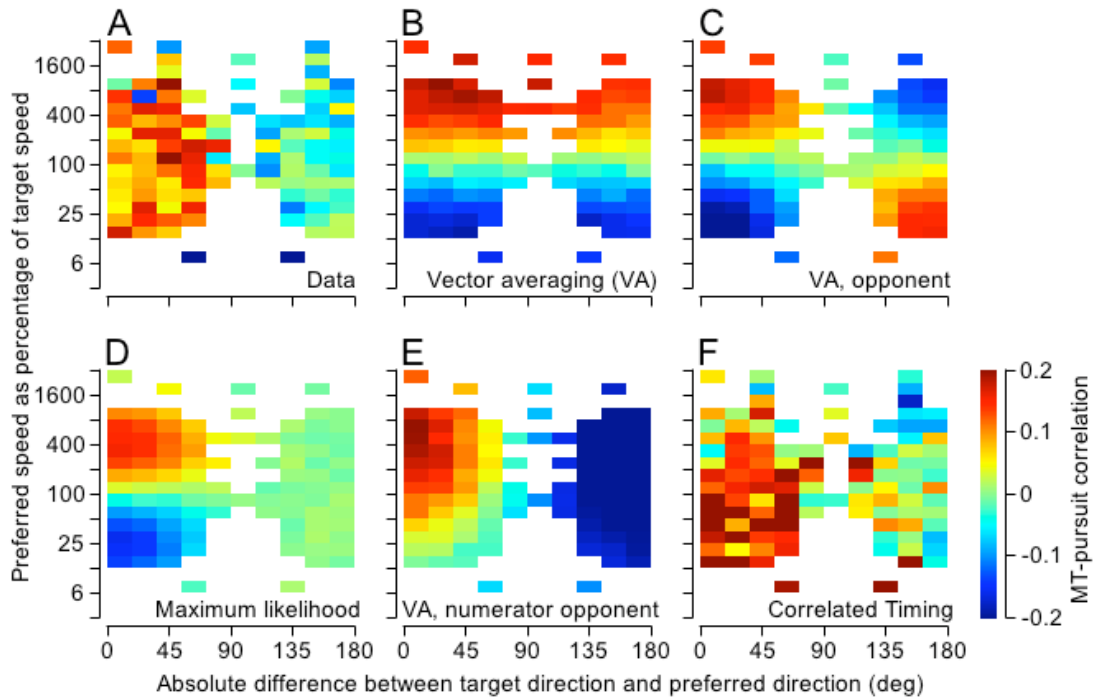


Figure 3.6.

MT-pursuit correlation structure of the data (A, earliest pursuit interval) compared to the predictions of various decoding models (B-E) and the presence of correlated timing (F). All panels show the value of correlation coefficients between firing rates and eye speed (i.e. speed readout) in color. Correlation coefficients are plotted against preferred speed as a percentage of target speed along the vertical axis and the difference between preferred and target direction along the horizontal axis. The model corresponding to each predicted correlation structure is indicated at the bottom of each panel. The correlation coefficients

shown are averages across all data points falling into a given bin. For the ‘data’ and ‘correlated timing’ panels correlation coefficients are averaged across both monkeys.

A vector averaging decoding model with direction opponency only in the numerator predicted the MT-pursuit correlation structure that most closely resembled our data (Figure 3.6E). There still were some differences, for example the relatively low MT-pursuit correlations predicted for model neurons with low preferred speeds and preferred directions within 90 degrees of target direction, and the large magnitude of the negative correlations for model neurons with preferred directions that differed from target direction by more than 90 degrees. In this model, the numerator is the same as for opponent vector averaging, but all neurons contribute to the denominator in a positive manner independent of their preferred directions. The presence of opponency only in the numerator effectively decouples any interaction between the numerator and the denominator. In the standard and opponent vector averaging decoders, in contrast, the interaction between the numerator and denominator is responsible for the speed dependency of the predicted MT-pursuit correlations. The most striking feature of our MT-pursuit correlation data is the absence of this speed dependency (Figure 3.5D, E, F).

Our analysis is based on the well-supported premise that there is a sensory source of pursuit variation, that the source resides in correlated noise in MT responses, and that the correlated noise is of an appropriate structure and amplitude to lead to the observed variation in the initiation of pursuit (Huang & Lisberger, 2009; Medina & Lisberger, 2007; Osborne et al., 2005; Schoppik et al., 2008). If, in spite of these findings, we assume that the variation in pursuit arises downstream from the locus where the

representation of motion in MT is decoded to estimate target direction and speed, then there is an alternative explanation for our data. Suppose that the latency of onset of MT responses and pursuit eye velocity are variable from trial to trial and that they shift to some degree together. Because we are analyzing firing rate and eye velocity in a fixed temporal window relative to the onset of target motion, coordinated latency shifts would cause MT-pursuit correlations. As shown in figure 3.6F, the structure of the MT-pursuit correlations predicted by the time shift hypothesis is qualitatively similar to that seen in our data. We will return to this issue in the Discussion.

Correlations between neurons in the MT population are necessary for observing MT-pursuit correlations of the magnitude of those we measured in our data. Figure 3.7 shows the same decoders as in figure 3.6 applied to a simulated population of MT units with the same properties as the population in figure 3.6, except that the noise of each unit is independent of the noise of all other units. As can be seen, MT-pursuit correlations are nearly non-existent without correlated noise in the MT population.

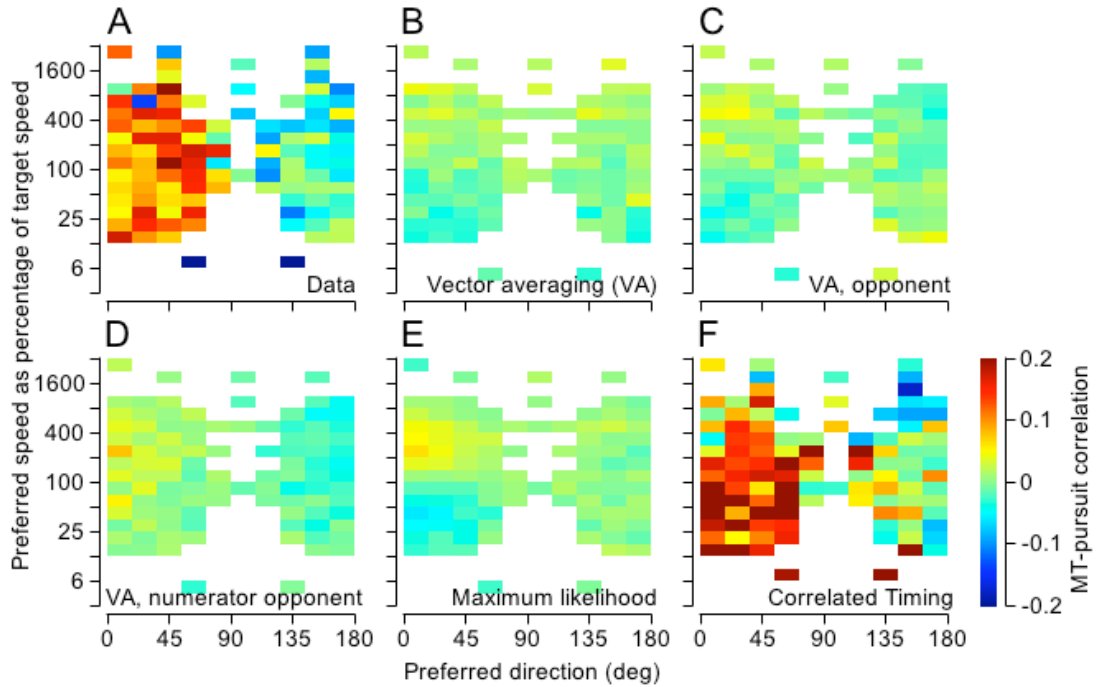


Figure 3.7.

Predicted MT-pursuit correlations plotted as in figure 3.6 resulting from an MT population without neuron-neuron correlations between units. The MT-pursuit correlations for the data and the prediction of the correlated timing are identical as in figure 3.6 because they are not based on the simulated MT population and serve as reference. For ease of comparison we left the scale of the colorbar the same as in figure 3.6.

Noise Reduction

Individual MT neurons are noisy with a variance approximately equal to their mean spike count (Churchland et al., 2010). The standard doctrine is that averaging

across neurons reduces the noise in the behavior driven by MT responses, while noise correlations among neurons limit the noise reduction (Shadlen et al., 1996). Thus, noise reduction provides a complement to MT-pursuit correlations in our attempt to establish the sources of variation in pursuit behavior and the mechanisms that transform the MT population response into estimates of target velocity for driving the initiation of pursuit. To explore this axis of our data and the predictions of the different decoding computations, we have analyzed the amount of noise reduction between the response of each MT neuron in our sample and the associated eye movements.

To compare neural to behavioral noise, it was necessary to convert eye speed into the same units as firing rate. For each trial in the collection of responses to a single target motion, we converted eye speed 100 ms after the onset of pursuit to an estimate of target speed as:

$$\dot{T}'_i = \frac{\dot{E}_i(t = 100)}{\dot{E}(t = 100)} \dot{T} \quad (16)$$

where the dots over the symbols indicate speed, T and E refer to the target and the eye, i indexes the trials, and the denominator is the mean across all trials. Then, we converted the estimate of target speed for each trial to the units of firing rate by projecting through the mean speed tuning curve for the neuron under study, as illustrated in figure 3.8A. We performed this analysis only for MT neurons with preferred directions within 90 degrees of the direction of target motion.

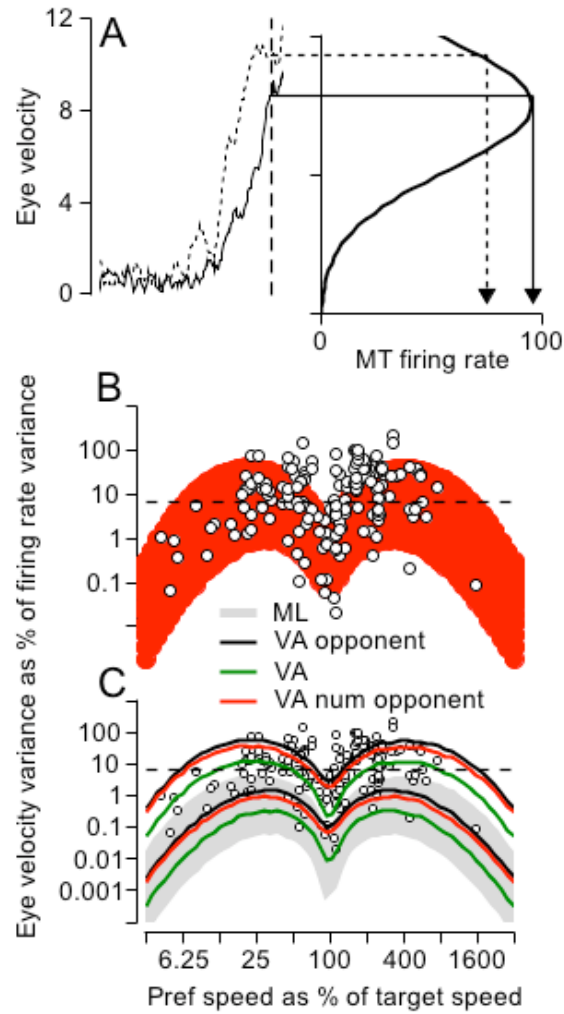


Figure 3.8.

Noise reduction between single neurons in MT and pursuit eye speed. **A, left:** Eye speed is converted to an estimate of target speed by comparing it to the mean response (equation 16). **A, right:** Speed estimate is converted into units of firing rate by using the speed-tuning curve. We computed variance reduction for eye speed 200ms after motion onset. The tuning curve is based on firing rates 25-140ms after motion onset, the time interval relevant for guiding the eyes at 200ms. **B:** Noise reduction between eye speed and firing rate for each

cell, trial condition, and both monkeys. Noise reduction is plotted as a function of preferred speed in percent of target speed. Data is included only for trial conditions in which the difference between preferred and target direction was less than 90 degrees. C: predicted noise reduction of each decoder. ML: maximum likelihood. VA opponent: opponent vector averaging. VA: vector averaging. VA num opponent: vector averaging with opponent numerator.

The variance of eye speed, transformed into units of spikes/s as outlined above, clustered around 10% of the variance of firing rate across our sample of MT neurons (Figure 3.8B, open symbols). Simple averaging of N independent neurons would predict a noise reduction of $1/N$, so the improvement in variance would be expected to be much larger for simple, linear averaging of the MT population responses. Given that all practical decoding models are highly non-linear, we performed the same analysis of the data obtained from the computer simulations used to create figure 3.6.

Each model produced a range of values of noise reduction at each value of preferred speed, because of the different response amplitudes and variances of neurons with different preferred directions. The predicted noise reduction agreed well with the data for the vector averaging model with opponency in the numerator (red band in figure 3.8B, area delimited by red curves in figure 3.8C). Figure 3.8C shows that the noise reduction was similar for the fully opponent vector averaging decoder (black curves) and the numerator opponent vector averaging model (red curves). Noise reduction was better for the standard vector averaging model (green curves) and best for the maximum likelihood model (light gray shading). The two opponent vector averaging models made

predictions that agreed well with our MT recordings, while the maximum likelihood decoder predicted noise reduction that exceeded what we measured.

Discussion

We found that under identical stimulus conditions, trial-by-trial fluctuations in the activity of single neurons in visual area MT are correlated with variation in eye speed at pursuit initiation. Our results are a strong indication that fluctuations in MT responses contribute to variation in the motor output. Although correlations do not prove causality, our interpretation is motivated by the fact that the initiation of smooth pursuit eye movements relies on signals from MT (Lisberger, 2010; Newsome, Wurtz, Dursteler, & Mikami, 1985). The MT-pursuit correlations were strongest and positive when the target moved in the preferred direction of the neurons and slightly negative when the targets moved in the opposite direction. Simulation of a population of MT neurons showed that this correlation structure is consistent with a modified vector averaging readout containing an opponent structure between neurons with opposite direction tuning. Further, we found that the variance in eye speed is approximately a tenth of the variance of single MT neurons during pursuit initiation. Considering the large number of MT neurons that could be read out by downstream areas, the difference in variance observed between single sensory neurons and the motor output is quite small.

Assuming a fixed number of neurons contributing to the readout, there are two possible explanations for the small difference in variance between MT neurons and eye speed. First, pooling MT responses could effectively eliminate sensory noise and the noise in the motor behavior would thus arise purely from downstream areas. Second, shared noise cannot be removed by pooling neural responses because of the presence of weak neuron-neuron correlations in MT (Bair, Zohary, & Newsome, 2001; Huang &

Lisberger, 2009) and therefore the noise propagates across synapses, contributing to fluctuations in the motor output. The first explanation is inconsistent with the observed strong MT-pursuit correlations, while the second explanation agrees with our findings. This implies that errors in sensory estimation of speed lead to the formation of an imprecise motor command on individual trials. Considering that signals must travel across multiple synapses from MT to reach the motor neurons, it is remarkable that fluctuations in individual sensory neurons co-vary with the motor behavior. Our conclusions are in line with the results of previous studies that have suggested that motor noise has a sensory source for pursuit eye movements (Medina & Lisberger, 2007; Osborne et al., 2005; Schoppik et al., 2008).

The structure of MT-pursuit correlations can be interpreted in several ways, depending on the assumptions made about noise added downstream from MT. We first discuss the possibility that no noise is added downstream from MT, consistent with the findings of several previous studies (Huang & Lisberger, 2009; Medina & Lisberger, 2007; Osborne et al., 2005; Schoppik et al., 2008). If downstream noise is nearly non-existent, simulations of a realistic MT population have shown that various aspects of smooth pursuit eye movements naturally arise from the properties of the neural population in MT. These include accounting for the mean and the variance of eye speed (Churchland & Lisberger, 2001; Huang & Lisberger, 2009; Priebe & Lisberger, 2004), and the magnitude of MT-pursuit correlations we measured. In this scenario, the structure of MT-pursuit correlations informs us about how speed is read out from MT by constraining possible decoding mechanisms of the population of MT neurons.

Our simulations showed that different models for decoding speed from MT make specific predictions about the expected structure of MT-pursuit correlations as a function of the tuning properties of the MT neurons. Of the decoders we tested, only a modified form of vector averaging, including direction-opponency, could reproduce the pattern of MT-pursuit correlations seen in the experimental data. In contrast to other implementations of vector averaging, this decoder computes an approximation of, rather than the exact center of mass of the neural population. As a consequence, the resulting MT-pursuit correlations are nearly flat as a function of the preferred speeds of the neurons, similar to what we observed in our data.

The measured pattern of MT-pursuit correlations appears inconsistent with a readout mechanism that has optimal precision. Previous work on optimal decoding has suggested that the contribution of a sensory neuron to a perceptual estimate depends on the nature of the task and on the relationship between the neuron's tuning preferences and the properties of the stimulus (Jazayeri & Movshon, 2006). For example, in a two-alternative direction discrimination task, the difference in the angle between the two alternatives determines which neurons contribute most to the estimate of direction. The largest contribution comes from the most responsive neurons for coarse discriminations, while fine discriminations depend on neurons that are stimulated on the flanks of their tuning curves (Britten et al., 1996; Cohen & Newsome, 2009; Jazayeri & Movshon, 2006; Purushothaman & Bradley, 2005). In the case of pursuit, the brain must identify the correct speed of the target stimulus from a continuum, rather than discriminating between a few discrete speeds. The maximum likelihood solution to this problem predicts that neurons stimulated at the flanks of their speed tuning curves should contribute most to the

speed readout, as in fine discriminations. Our data, however, are inconsistent with this theoretical prediction, as we found no effect of preferred speed on MT-pursuit correlations.

The discrepancy between the observed correlations and the prediction of an optimal readout might reflect a fundamental difference between slow perceptual decisions that allow a subject to integrate evidence over as much as seconds, and fast motor responses that are initiated within less than 100 milliseconds. In the case of pursuit initiation, the first spikes after motion onset might provide only a rough, sub-optimal estimate of speed that is used for an inexact, but quick initiation of movement. Consistent with this idea, the variance of the pursuit response is high at the onset of pursuit initiation (Osborne et al., 2007). Fast motor responses, unlike perceptual decisions, might thus inherently prioritize speed over precision at least until an initial estimate of the required sensory parameters is obtained.

If we instead suppose, in contrast to the assumptions made so far, that substantial noise is added downstream from MT, and that the decoder and the downstream noise fulfill specific requirements, then there is an alternative explanation for the structure of MT-pursuit correlations. This structure could arise from correlations in the latencies of the neural and behavioral responses. In this case, the latencies of neural responses in MT would have to be correlated with each other, so that temporal fluctuations in the onset of the neural responses would propagate to influence the timing of pursuit initiation. In addition, the noise added downstream would have to be of an appropriate magnitude to explain the variance in the behavior, as well as being low dimensional, spanning the dimensions of latency, speed, and direction to match the properties of noise during

pursuit initiation (Osborne et al., 2005). Moreover, the noise would have to originate upstream from the FEF and the cerebellum as previous studies have shown that very little noise is added downstream from these areas during pursuit initiation (Medina & Lisberger, 2007; Schoppik et al., 2008).

Although it is possible that timing contributes to MT-pursuit correlations to some degree, it seems implausible that the entire structure of neuron-behavior correlations arises from correlated latencies, because it is unlikely that downstream noise would fulfill all the constraints outlined above. Even if latency contributed to the observed correlations, this contribution would be difficult to tease apart from that of the decoder for several reasons. Ideally, to eliminate any effects of latency on MT-pursuit correlations, the neural and behavioral data should be realigned to response onset on a trial-by-trial basis before computing correlations. However, this would require estimates of the latency of pursuit and MT response onset of far greater accuracy than can be achieved in practice. In addition, it is likely that the latency and magnitude of neural responses are correlated with each other and that the effects of each cannot be considered separately. For example, strong, depolarizing membrane potentials will lead to both high firing rates and short response latencies producing correlations in time and magnitude of the neural response. Moreover, during pursuit initiation, the motor response itself contains correlations between the latency and speed of the eye movements (Osborne et al., 2005), which cannot be removed.

The MT-pursuit correlations in our task likely arise due to feed-forward propagation of neural variability from MT to the motor output. We measured the largest correlations in a 40 ms time window at the very beginning of the neural and behavioral

responses. During this time, MT responses are independent of the attentional state of the subject, as modulation of firing rates by attention does not occur until later in the neural response (Cook & Maunsell, 2004). Therefore, MT-pursuit correlations cannot be attributed to changes in attention on different trials throughout the experiment. We cannot, however, exclude the contribution of other cognitive factors to MT-pursuit correlations, like the overall level of alertness, as long as these affect the onset of the neural and behavioral responses. In contrast to our task, much longer timescales, usually on the order of seconds, have been used to link neural activity in MT to upcoming decisions in perceptual tasks. Although neuron-behavior correlations in that case might well be driven by feed-forward signals, attentional modulations potentially could contribute to correlations as has been suggested recently, because later time points of the response are included in the analysis (Cohen & Newsome, 2009; Nienborg & Cumming, 2009).

Our findings demonstrate that neuron-behavior correlations provide important information about the contribution of a brain area to a particular behavior. Knowledge about neuron-behavior correlations constrains possible decoding models beyond their ability to replicate the mean and variance of a perceptual task or motor behavior. Ultimately, analogous experiments measuring neuron-neuron and neuron-behavior correlations across different areas will be necessary to understand how a final behavior emerges from local computations along a given neural pathway.

References

- Albright, T. D. (1984). Direction and orientation selectivity of neurons in visual area MT of the macaque. *J Neurophysiol*, 52(6), 1106-1130.
- Bair, W., Zohary, E., & Newsome, W. T. (2001). Correlated firing in macaque visual area MT: time scales and relationship to behavior. *J Neurosci*, 21(5), 1676-1697.
- Britten, K. H., Newsome, W. T., Shadlen, M. N., Celebrini, S., & Movshon, J. A. (1996). A relationship between behavioral choice and the visual responses of neurons in macaque MT. *Vis Neurosci*, 13(1), 87-100.
- Britten, K. H., Shadlen, M. N., Newsome, W. T., & Movshon, J. A. (1992). The analysis of visual motion: a comparison of neuronal and psychophysical performance. *J Neurosci*, 12(12), 4745-4765.
- Churchland, M. M., Afshar, A., & Shenoy, K. V. (2006). A central source of movement variability. *Neuron*, 52(6), 1085-1096.
- Churchland, M. M., & Lisberger, S. G. (2001). Shifts in the population response in the middle temporal visual area parallel perceptual and motor illusions produced by apparent motion. *J Neurosci*, 21(23), 9387-9402.
- Churchland, M. M., Yu, B. M., Cunningham, J. P., Sugrue, L. P., Cohen, M. R., Corrado, G. S., et al. (2010). Stimulus onset quenches neural variability: a widespread cortical phenomenon. *Nat Neurosci*, 13(3), 369-378.

- Cohen, M. R., & Newsome, W. T. (2009). Estimates of the contribution of single neurons to perception depend on timescale and noise correlation. *J Neurosci*, *29*(20), 6635-6648.
- Cook, E. P., & Maunsell, J. H. (2004). Attentional modulation of motion integration of individual neurons in the middle temporal visual area. *J Neurosci*, *24*(36), 7964-7977.
- Deneve, S., Latham, P. E., & Pouget, A. (1999). Reading population codes: a neural implementation of ideal observers. *Nat Neurosci*, *2*(8), 740-745.
- Desimone, R., & Ungerleider, L. G. (1986). Multiple visual areas in the caudal superior temporal sulcus of the macaque. *J Comp Neurol*, *248*(2), 164-189.
- Dodd, J. V., Krug, K., Cumming, B. G., & Parker, A. J. (2001). Perceptually bistable three-dimensional figures evoke high choice probabilities in cortical area MT. *J Neurosci*, *21*(13), 4809-4821.
- Faisal, A. A., Selen, L. P., & Wolpert, D. M. (2008). Noise in the nervous system. *Nat Rev Neurosci*, *9*(4), 292-303.
- Groh, J. M. (2001). Converting neural signals from place codes to rate codes. *Biol Cybern*, *85*(3), 159-165.
- Groh, J. M., Born, R. T., & Newsome, W. T. (1997). How is a sensory map read Out? Effects of microstimulation in visual area MT on saccades and smooth pursuit eye movements. *J Neurosci*, *17*(11), 4312-4330.
- Harris, C. M., & Wolpert, D. M. (1998). Signal-dependent noise determines motor planning. *Nature*, *394*(6695), 780-784.

- Huang, X., & Lisberger, S. G. (2009). Noise correlations in cortical area MT and their potential impact on trial-by-trial variation in the direction and speed of smooth-pursuit eye movements. *J Neurophysiol*, *101*(6), 3012-3030.
- Jazayeri, M., & Movshon, J. A. (2006). Optimal representation of sensory information by neural populations. *Nat Neurosci*, *9*(5), 690-696.
- Krauzlis, R. J. (2004). Recasting the smooth pursuit eye movement system. *J Neurophysiol*, *91*(2), 591-603.
- Lagae, L., Raiguel, S., & Orban, G. A. (1993). Speed and direction selectivity of macaque middle temporal neurons. *J Neurophysiol*, *69*(1), 19-39.
- Leopold, D. A., & Logothetis, N. K. (1996). Activity changes in early visual cortex reflect monkeys' percepts during binocular rivalry. *Nature*, *379*(6565), 549-553.
- Lisberger, S. G. (2010). Visual guidance of smooth-pursuit eye movements: sensation, action, and what happens in between. *Neuron*, *66*(4), 477-491.
- Lisberger, S. G., & Ferrera, V. P. (1997). Vector averaging for smooth pursuit eye movements initiated by two moving targets in monkeys. *J Neurosci*, *17*(19), 7490-7502.
- Lisberger, S. G., Morris, E. J., & Tychsen, L. (1987). Visual motion processing and sensory-motor integration for smooth pursuit eye movements. *Annu Rev Neurosci*, *10*, 97-129.
- Lisberger, S. G., & Movshon, J. A. (1999). Visual motion analysis for pursuit eye movements in area MT of macaque monkeys. *J Neurosci*, *19*(6), 2224-2246.

- Lisberger, S. G., & Westbrook, L. E. (1985). Properties of visual inputs that initiate horizontal smooth pursuit eye movements in monkeys. *J Neurosci*, 5(6), 1662-1673.
- Logothetis, N. K., & Schall, J. D. (1989). Neuronal correlates of subjective visual perception. *Science*, 245(4919), 761-763.
- Maunsell, J. H., & Van Essen, D. C. (1983). Functional properties of neurons in middle temporal visual area of the macaque monkey. I. Selectivity for stimulus direction, speed, and orientation. *J Neurophysiol*, 49(5), 1127-1147.
- Medina, J. F., & Lisberger, S. G. (2007). Variation, signal, and noise in cerebellar sensory-motor processing for smooth-pursuit eye movements. *J Neurosci*, 27(25), 6832-6842.
- Newsome, W. T., Britten, K. H., & Movshon, J. A. (1989). Neuronal correlates of a perceptual decision. *Nature*, 341(6237), 52-54.
- Newsome, W. T., Wurtz, R. H., Dursteler, M. R., & Mikami, A. (1985). Deficits in visual motion processing following ibotenic acid lesions of the middle temporal visual area of the macaque monkey. *J Neurosci*, 5(3), 825-840.
- Nienborg, H., & Cumming, B. G. (2009). Decision-related activity in sensory neurons reflects more than a neuron's causal effect. *Nature*, 459(7243), 89-92.
- Osborne, L. C., Hohl, S. S., Bialek, W., & Lisberger, S. G. (2007). Time course of precision in smooth-pursuit eye movements of monkeys. *J Neurosci*, 27(11), 2987-2998.

- Osborne, L. C., Lisberger, S. G., & Bialek, W. (2005). A sensory source for motor variation. *Nature*, 437(7057), 412-416.
- Priebe, N. J., Churchland, M. M., & Lisberger, S. G. (2001). Reconstruction of target speed for the guidance of pursuit eye movements. *J Neurosci*, 21(9), 3196-3206.
- Priebe, N. J., & Lisberger, S. G. (2004). Estimating target speed from the population response in visual area MT. *J Neurosci*, 24(8), 1907-1916.
- Purushothaman, G., & Bradley, D. C. (2005). Neural population code for fine perceptual decisions in area MT. *Nat Neurosci*, 8(1), 99-106.
- Ramachandran, R., & Lisberger, S. G. (2005). Normal performance and expression of learning in the vestibulo-ocular reflex (VOR) at high frequencies. *J Neurophysiol*, 93(4), 2028-2038.
- Rashbass, C. (1961). The relationship between saccadic and smooth tracking eye movements. *J Physiol*, 159, 326-338.
- Ress, D., & Heeger, D. J. (2003). Neuronal correlates of perception in early visual cortex. *Nat Neurosci*, 6(4), 414-420.
- Rodman, H. R., & Albright, T. D. (1987). Coding of visual stimulus velocity in area MT of the macaque. *Vision Res*, 27(12), 2035-2048.
- Salinas, E., & Abbott, L. F. (1994). Vector reconstruction from firing rates. *J Comput Neurosci*, 1(1-2), 89-107.

- Schoppik, D., Nagel, K. I., & Lisberger, S. G. (2008). Cortical mechanisms of smooth eye movements revealed by dynamic covariations of neural and behavioral responses. *Neuron*, *58*(2), 248-260.
- Shadlen, M. N., Britten, K. H., Newsome, W. T., & Movshon, J. A. (1996). A computational analysis of the relationship between neuronal and behavioral responses to visual motion. *J Neurosci*, *16*(4), 1486-1510.
- Snowden, R. J., Treue, S., & Andersen, R. A. (1992). The response of neurons in areas V1 and MT of the alert rhesus monkey to moving random dot patterns. *Exp Brain Res*, *88*(2), 389-400.
- Uka, T., & DeAngelis, G. C. (2004). Contribution of area MT to stereoscopic depth perception: choice-related response modulations reflect task strategy. *Neuron*, *42*(2), 297-310.
- van Beers, R. J., Haggard, P., & Wolpert, D. M. (2004). The role of execution noise in movement variability. *J Neurophysiol*, *91*(2), 1050-1063.
- Warland, D. K., Reinagel, P., & Meister, M. (1997). Decoding visual information from a population of retinal ganglion cells. *J Neurophysiol*, *78*(5), 2336-2350.
- Yang, J., & Lisberger, S. G. (2009). Relationship between adapted neural population responses in MT and motion adaptation in speed and direction of smooth-pursuit eye movements. *J Neurophysiol*, *101*(5), 2693-2707.

Zohary, E., Celebrini, S., Britten, K. H., & Newsome, W. T. (1994). Neuronal plasticity that underlies improvement in perceptual performance. *Science*, 263(5151), 1289-1292.

Chapter 4: Appendix

Linear predictions of pursuit eye velocity

This appendix is a supplement to chapter 3 and provides further detail on the structure of the temporal autocorrelations in eye velocity around pursuit initiation and the construction of the linear predictions that we used to remove them. First, we show the magnitude of the fluctuations during fixation that give rise to deviations in pursuit eye velocity and then provide an example of a typical correlation structure for one experiment and stimulus condition. We further discuss how the predictions for pursuit eye velocity depend on the temporal parameters of the linear filter and show how we obtained the optimal parameters that we used to remove the autocorrelations in eye velocity.

Temporal correlations in eye velocity

Even under stringent fixation requirements, eye velocity is variable across identical repetitions of the same stimulus and across time during a single trial, both during fixation and pursuit initiation. An example of the variability in eye velocity during fixation and pursuit initiation is shown in figure 4.1 (left panel). Variability in eye velocity occurs naturally and cannot be suppressed. Fluctuations in eye velocity during fixation induce image velocity on the retina which can potentially alter the perception of motion in the pursuit target. We therefore only included trials in our analysis that were free of saccades or microsaccades. The remaining eye movements during fixation are tremor and drifts as described in chapter 2 and are small in amplitude (Martinez-Conde, Macknik, & Hubel, 2004). Despite the fact that in our data deviations in eye velocity are small during fixation, these movements give rise to fluctuations in eye velocity of similar magnitude during pursuit initiation (Figure 4.1, right panel).

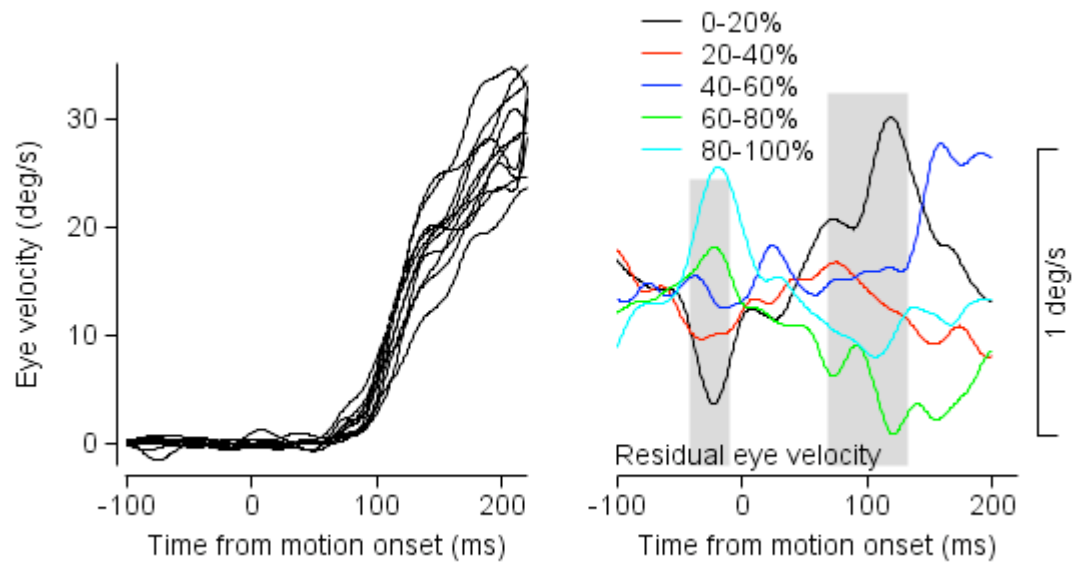


Figure 4.1.

Variability in eye velocity during fixation and pursuit. Left panel: Typical smooth pursuit eye movement traces in response to repeated presentation of an identical pursuit stimulus. Eye speed along the direction of target motion is plotted against time. Right panel: Residual eye velocity (i.e. deviations from mean eye velocity) in the direction of target motion as a function of time. Trials were grouped and averaged according to magnitude of residual speed before motion onset (first gray bar). The second gray bar indicates the time of pursuit onset.

Pursuit eye velocity is correlated with eye velocity during fixation predominantly in the direction of target motion which is also the direction in which the eyes move during pursuit. Our pursuit stimulus moved on a two-dimensional screen located in front of the subject. In order to look at temporal correlations, we divided up eye velocity into a component parallel and orthogonal to the direction of target motion. For eye speed parallel to target motion, the initial pursuit response was negatively correlated with eye speed immediately before the onset of motion in the stimulus (Figure 4.2, left panel). This correlation was strongest at the onset of pursuit and decayed with time throughout pursuit initiation. In addition to the negative correlation, pursuit eye speed was positively correlated with fixation eye speed approximately 100 ms before motion onset. The oscillation between positive and negative correlations throughout fixation is due to the oscillatory nature of drifts in eye movements described in chapter 2. For eye velocity orthogonal to stimulus direction, there is little correlation between eye speed during fixation and pursuit. This is expected as the eyes hardly move along this direction (Figure 4.2, right panel).

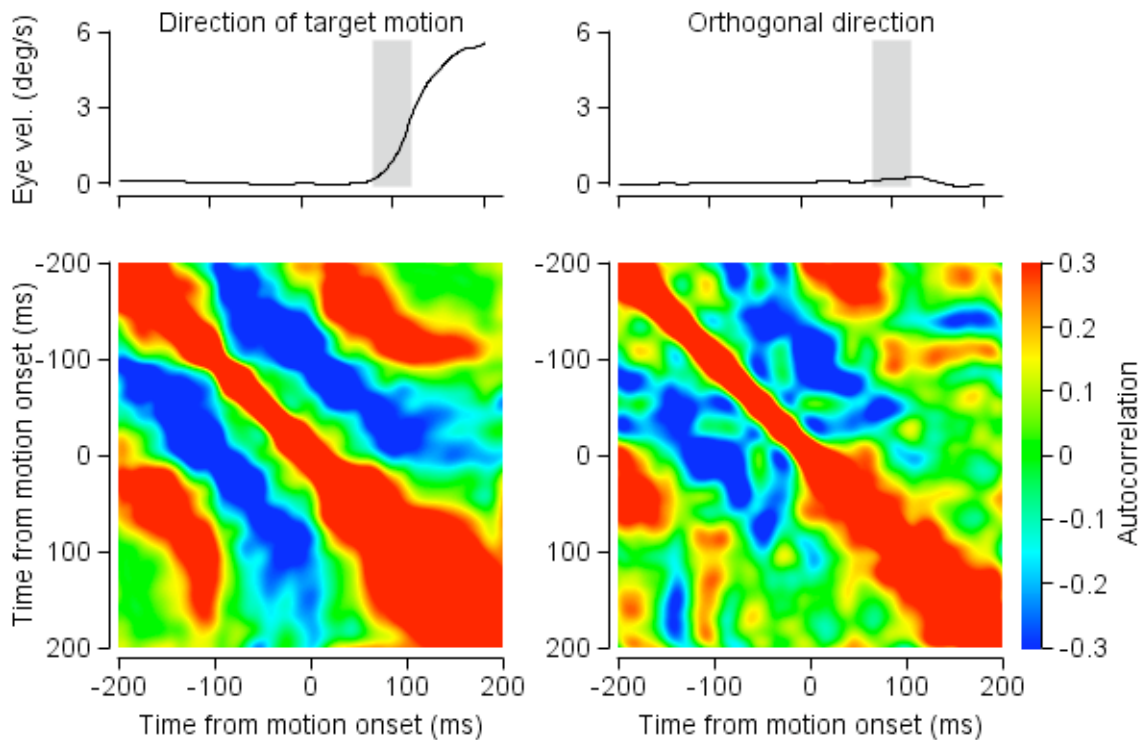


Figure 4.2.

Typical correlation matrix of eye speed parallel (left) and orthogonal (right) to stimulus direction for a single target motion during one experiment. Each pixel shows the correlation coefficient between eye speed at two different time points which are indicated on the horizontal and vertical axes. Trials are aligned to target motion onset at 0ms. For reference we plotted the mean eye speed in the corresponding direction above each correlation matrix. Pursuit is initiated 80-100 ms after motion onset.

Predicting pursuit eye velocity

We constructed linear filters for predicting pursuit from fixation eye velocity by using methods that have been applied to similar problems (Warland, Reinagel, & Meister, 1997). To find the best prediction of pursuit velocity we first divided up eye velocity into

components parallel and orthogonal to target motion and then explored the temporal parameters used to create the filter and thereby the pursuit predictions. We outlined the derivation of the filters in chapter 3 and briefly repeat the equations below:

\mathbf{V}_{fix} - matrix describing eye velocity during fixation with trials in rows and time points in columns

v_j^i - eye speed in direction of target motion for trial i and time point j

ov_j^i - eye speed orthogonal to target direction for trial i and time point j

\mathbf{V}_{purs} - pursuit eye velocity (either parallel or orthogonal to target motion)

$\mathbf{V}_{\text{purs}}^{\text{pred}}$ - predicted pursuit eye velocity (either parallel or orthogonal to target motion, same direction as \mathbf{V}_{purs})

$$\mathbf{V}_{\text{fix}} = \begin{bmatrix} v_1^1 & v_2^1 & \cdots & v_n^1 & ov_1^1 & ov_2^1 & \cdots & ov_n^1 \\ v_1^2 & v_2^2 & \cdots & v_n^2 & ov_1^2 & ov_2^2 & \cdots & ov_n^2 \\ \vdots & \vdots & \ddots & \vdots & \vdots & \vdots & \ddots & \vdots \\ v_1^m & v_2^m & \cdots & v_n^m & ov_1^m & ov_2^m & \cdots & ov_n^m \end{bmatrix}, \mathbf{V}_{\text{purs}} = \begin{bmatrix} v_p^1 \\ v_p^2 \\ \vdots \\ v_p^m \end{bmatrix}$$

First we calculated the filter \mathbf{f} describing the relationship between pursuit and fixational eye velocity and then used it to obtain the prediction of pursuit velocity:

$$\mathbf{f} = (\mathbf{V}_{\text{fix}}^T \mathbf{V}_{\text{fix}})^{-1} \cdot (\mathbf{V}_{\text{fix}}^T \mathbf{V}_{\text{purs}}) \quad (1)$$

$$\mathbf{V}_{\text{purs}}^{\text{pred}} = \mathbf{V}_{\text{fix}} \cdot \mathbf{f} \quad (2)$$

The prediction of pursuit eye velocity is the solution to a multilinear regression between fixation and pursuit eye velocity. The independent variables of the regression

consist of the time points of eye velocity during fixation while pursuit eye velocity makes up the dependent variable. As described in chapter 3, we minimized correlations between the independent variables by downsampling eye velocity by 20ms. Subtracting the predicted from actual pursuit velocity, as we did in chapter 3 and using the equations above, removes correlations between fixation and the residual portion of pursuit eye velocity.

Evaluating linear predictions of pursuit eye speed

For evaluating the predictive power of the linear filters, we derived filters based on two thirds of the trials for each experiment and tested the predictions on the remaining third of the trials. We used the coefficient of determination to obtain the percent of variance of the actual pursuit speed that is explained by the predicted pursuit speed.

$$\text{Percent of variance explained} = 100 * \left(1 - \frac{\sum_i (y_i^{actual} - y_i^{pred})^2}{\sum_i (y_i^{actual} - \overline{y^{actual}})^2} \right) \quad (3)$$

The coefficient of determination has no lower bound and takes on negative values when the linear prediction is inadequate. We therefore replaced negative values with zeros before computing averages across experiments, because in that case the model has no predictive power and zero percent of variance is explained by the prediction.

Across experiments the predictions of pursuit velocity depended on temporal parameters in a stereotyped manner consistent with our observation that the correlation structure of eye velocity was similar across experiments. We evaluated the predictions by

changing both which and how many time points of fixation were included to derive the filter (equation 1). Because the temporal structure of the predictions did not depend on the target speed or direction used in a particular experiment, we averaged the percent of variance explained by the prediction across all experiments, stimulus conditions, and monkeys (Figure 4.3).

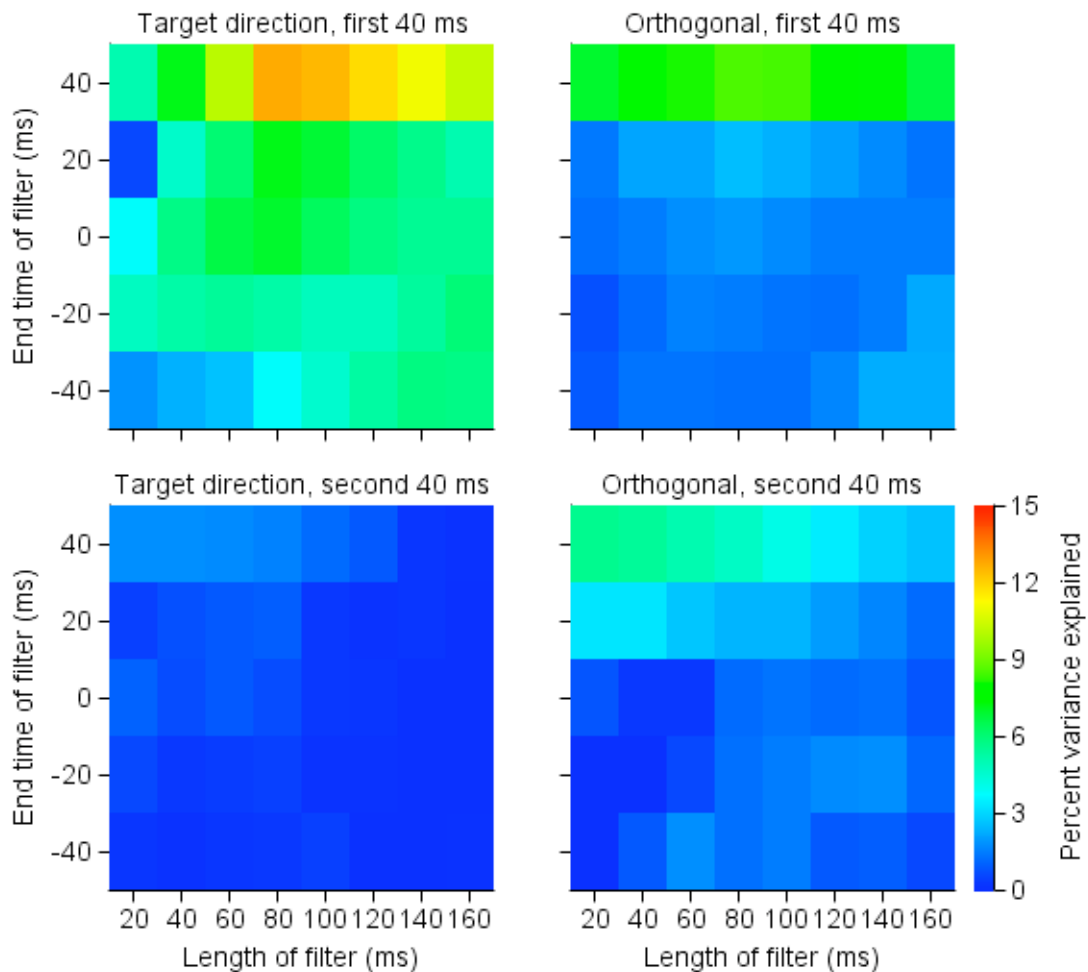


Figure 4.3.

Percent of variance of pursuit eye speed predicted by eye speed during fixation. Top row: Variance explained for pursuit 80-120 ms after motion onset. Percent of variance is indicated in color and for each set of temporal parameters was averaged across experiments, target motions, and monkeys and shown in color. The vertical axis indicates the end time of the filter (i.e. the last time point of fixation considered). The horizontal axis describes the length of the filter (i.e. how many time points of fixation were used to calculate the filters). Left column: percent of pursuit variance explained for speed in target direction. Right column: percent of pursuit variance explained for speed orthogonal to target direction. Bottom row: Variance explained for pursuit 120-160 ms after motion onset. Filters were computed on velocity that was downsampled by 20ms and 0 ms indicates the time of motion onset in the stimulus.

The linear predictions of pursuit reflected several features of the correlation structure in eye velocity shown in figure 4.2: First, filters including time points right before motion onset were most predictive of pursuit eye velocity. This is consistent with the existence of substantial negative correlations between eye speed before motion onset and during pursuit initiation. Second, when time points closer to pursuit onset were included in the filter, the predictions were more accurate. This is simply a reflection of the correlations between fixation and pursuit decaying with greater temporal lags. Third, predictions were more accurate for eye velocity in the direction parallel rather than orthogonal to target motion. This is unsurprising because almost all of the motion of the eyes was in the direction of target motion and correlations were weaker for motion orthogonal rather than parallel to target motion. Lastly, the largest proportion of pursuit speed that could be explained was for the first interval of pursuit initiation, 80–120 ms

after motion onset. Later time intervals of pursuit were less correlated with fixational eye movements and, on average, filters had little predictive power later throughout pursuit initiation.

For speed in the direction of target motion and pursuit at 80-120ms after motion onset, the optimal filter was 80ms in length and took into account time points from -40ms to +40ms around motion onset. On average, it predicted $12.7\% \pm 6.4\%$ of pursuit variance across all experiments and target motions. For speed orthogonal to the direction of motion and using the same filter parameters the linear predictions explained $8.6\% \pm 6.0\%$ of pursuit variance. For speed 120-160ms after motion onset, filters predicted only 2.2% and 2.6% of pursuit variance for motion parallel and orthogonal to target direction when we used the same temporal parameters as above. The predictive power of the filters was negligible further into pursuit initiation (data not shown).

In summary, given that the optimal filter was based on fixation at least 40ms before the beginning of the pursuit response, we were able to show that significant long-range temporal correlations exist between eye speed during fixation and pursuit initiation. We have shown that a small but significant fraction of pursuit speed can be predicted by fluctuations of the eyes during fixation.

References

Martinez-Conde, S., Macknik, S. L., & Hubel, D. H. (2004). The role of fixational eye movements in visual perception. *Nat Rev Neurosci*, 5(3), 229-240.

Warland, D. K., Reinagel, P., & Meister, M. (1997). Decoding visual information from a population of retinal ganglion cells. *J Neurophysiol*, 78(5), 2336-2350.

Chapter 5: Conclusions and Future Directions

In this thesis we investigated interactions between the processing of visual and oculomotor signals by analyzing responses in visual area MT during different types of eye movements. Our neural recordings showed that cells in visual area MT are exquisitely sensitive to small changes in image velocity caused by eye movements during fixation. In turn, small fluctuations in firing rates of individual MT neurons are predictive of deviations in eye speed at the initiation of smooth pursuit eye movements. These findings demonstrate that the neural mechanisms underlying sensory processing and the production of motor behavior are tightly interwoven.

The ability of the brain to produce high acuity vision and precise motor behavior in spite of the complex interactions between the sensory and motor systems is remarkable. First, the constant motion of the eyes requires the brain to convert an ever-changing retinal image into a stable perception of the world. Second, the brain must accurately extract information about the environment from the non-stationary visual signals provided by the retina. For example, parameters such as the speed and direction of an object must be retrieved in the presence of the global motion generated by eye movements. This is particularly important for behaviors such as smooth pursuit eye movements which rely on visual motion signals to produce precise motor outcomes (Lisberger & Westbrook, 1985). Our results strongly suggest that small changes in sensory responses lead to slightly different motor actions. Therefore small errors in the estimation of sensory parameters are likely of consequence for precise behaviors relying on sensory input. Our brain, however, masters the mutual interactions between the sensory and motor systems effortlessly, allowing us to generate precise actions in spite of the constantly changing retinal input.

Various different types of eye movements generate image motion on the retina and in principle a single mechanism could be responsible for stabilizing all motion signals due to eye movements. Our findings, however, suggest that different neural mechanisms are involved in eliminating retinal image motion elicited by the various eye movements. During saccadic eye movements, for example, visual perception is impaired and we are unaware of any retinal motion despite the high velocities and large retinal displacements produced by these eye movements. This phenomenon of visual impairment is termed saccadic suppression and is thought to arise due to decreases in neural responses for the duration of the saccade. Evidence of diminished firing rates has been found in visual area MT where a subpopulation of neurons is selectively silenced during saccades, but not under identical retinal image motion during passive viewing (Thiele, Henning, Kubischik, & Hoffmann, 2002). In contrast to saccades, drifts have a very different velocity profile. They are slow, small movements of low frequency content. We found that almost all MT neurons are modulated during drifts with no evidence of suppression of neural responses. Therefore other neural mechanisms that do not involve silencing of neurons must be involved in eliminating retinal image motion due to drifts.

Although we found that MT neurons carry signals during drifts that are potentially useful for perceptual stabilization of the visual world, many open questions remain as to how neural responses from various visual areas are combined to eliminate retinal motion due to eye movements. Studies using a visual illusion called the jitter illusion have shown that perceptual stabilization relies on visual signals due to image motion rather than extraretinal input about the eye movements. The jitter illusion takes advantage of adaptation of visual neurons to disrupt the neural mechanisms that stabilize

the retinal image during fixation. This disruption causes the subjects to see the image motion generated by their eye movements while they view a static visual stimulus. The development of a similar paradigm in primates where the subject could report the perception of motion would allow recordings of neural responses during normal vision and the perception of the illusion. Comparison of neural signals during normal vision and the perception of the illusion could provide deep insight into the visual areas and neural mechanisms involved in compensating for image motion generated by eye movements of fixation.

Neurons in visual area MT can be classified by their functional properties and it remains to be seen if the different cell types are involved in diverse mechanisms. In particular, MT neurons can be classified as being either component (CDS) or pattern direction selective (PDS) based on their responses to sinusoidal gratings and plaids. It is thought that the functional properties of PDS cells arise from an additional stage of motion processing within MT. In accordance with this theory, visual motion responses of CDS cells have been shown to have shorter latencies than those of PDS cells (Smith, Majaj, & Movshon, 2005). Short response latencies are essential for producing behaviors such as smooth pursuit eye movements, which require fast reaction times. It is therefore possible, that CDS neurons play an important role in initiating pursuit. Future experiments differentiating between different cell types will be necessary for elucidating whether, for example, CDS and PDS cells are both involved in and play different roles in producing smooth pursuit eye movements.

Our studies of MT have focused on the initiation of pursuit, which is the time during which smooth pursuit behavior relies only on visual motion input and feedback is

not yet available to correct for errors in the motor output (Lisberger, 2010; Lisberger & Westbrook, 1985). In contrast, extraretinal signals play an important role for the maintenance of pursuit when retinal image velocity of the pursuit target is small. In MT, a subpopulation of neurons responds substantially during ongoing pursuit even when the motion of the eyes closely matches target motion (Newsome, Wurtz, & Komatsu, 1988). The neural responses during this time period are thought to be elicited by retinal image motion due to the small discrepancies between eye and target motion. An interesting question arises as to whether the smooth pursuit system actively reads out these MT signals during the maintenance of pursuit to actively correct for errors in matching the motion of the eye to the speed and direction of the target.

Most areas involved in generating smooth pursuit eye movements are well known; their neural responses have been studied to explain their role in both the initiation and maintenance of pursuit. These studies have involved studying the effects of microstimulation and lesions, relating the mean and variance of neural responses to the mean and variance of the motor behavior, and finally quantifying neuron-behavior correlations to study sources of noise along the pursuit pathway and constrain existing models for pooling neural signals to generate pursuit behavior (Lisberger, 2010). Results from all these areas along the pursuit pathway can be combined to form a complete quantitative model for the generation of smooth pursuit behavior. Such a model would provide deep insight not only into the production of smooth pursuit eye movements but likely into the generation of a variety of sensory-motor behaviors in primates.

References

Lisberger, S. G. (2010). Visual guidance of smooth-pursuit eye movements: sensation, action, and what happens in between. *Neuron*, 66(4), 477-491.

Lisberger, S. G., & Westbrook, L. E. (1985). Properties of visual inputs that initiate horizontal smooth pursuit eye movements in monkeys. *J Neurosci*, 5(6), 1662-1673.

Newsome, W. T., Wurtz, R. H., & Komatsu, H. (1988). Relation of cortical areas MT and MST to pursuit eye movements. II. Differentiation of retinal from extraretinal inputs. *J Neurophysiol*, 60(2), 604-620.

Smith, M. A., Majaj, N. J., & Movshon, J. A. (2005). Dynamics of motion signaling by neurons in macaque area MT. *Nat Neurosci*, 8(2), 220-228.


Thiele, A., Henning, P., Kubischik, M., & Hoffmann, K. P. (2002). Neural mechanisms of saccadic suppression. *Science*, 295(5564), 2460-2462.

Publishing Agreement

It is the policy of the University to encourage the distribution of all theses, dissertations, and manuscripts. Copies of all UCSF theses, dissertations, and manuscripts will be routed to the library via the Graduate Division. The library will make all theses, dissertations, and manuscripts accessible to the public and will preserve these to the best of their abilities, in perpetuity.

Please sign the following statement:

I hereby grant permission to the Graduate Division of the University of California, San Francisco to release copies of my thesis, dissertation, or manuscript to the Campus Library to provide access and preservation, in whole or in part, in perpetuity.

 4/19/10
Author Signature Date